An engineering approach to the dynamic control of space robotic on-orbit servicers

A Ellery
Surrey Space Centre, University of Surrey, Guildford, Surrey, UK

Abstract: Robotic on-orbit servicing is the key to the commercial development of a space robotics infrastructure. A major technical difficulty has been the problem of control of the robotic manipulators mounted onto a freeflying platform in space. The problem of control is directly related to the fact that manipulator motions exert reaction effects on the mounting spacecraft. A solution to this problem is outlined—one in which no fuel is expended and that demands no excessive computational resources that would otherwise preclude real-time performance.

Keywords: in-orbit servicing, robotics, spacecraft, kinematics, dynamics, control

NOTATION

$\boldsymbol{a} = (a_x a_y a_z)^{\mathrm{T}}$	approach vector perpendicular to the end-effector palm (turn) for $i = n$
b_i	viscous friction on joint i
f_i	force on link i as a result of link $i-1$ supporting outboard links
$F_{\mathrm{c}i}$	total force on the link i centre of mass
F_{T}	total force acting at the manipulator base $(x_0 y_0 z_0)$ with respect to the base coordinates
F_0	total force acting at the manipulator base $(x_0 y_0 z_0)$ with respect to the inertial coordinates
$\boldsymbol{F}_{\mathrm{ext}} = (\boldsymbol{F}_{\mathrm{ext}} \boldsymbol{N}_{\mathrm{ext}})^{\mathrm{T}} = (F_x F_y F_z N_x N_y N_z)^{\mathrm{T}}$	generalized external Cartesian forces acting on the end-effector
i	link number from 0 to n
$\mathbf{I}_i$	3×3 inertia matrix of link i
$\boldsymbol{l}_i = \boldsymbol{r}_i + \boldsymbol{s}_i = (p_i - p_i - 1)$	vectorial length of link i from $(x_{I-1} y_{I-1} z_{I-1})$ to $(x_i y_i z_i)$
$\boldsymbol{L}$	angular momentum of the system
m_i	mass of each component rigid body i comprising the system
$\sum_{i=0}^{n+1} m_i = m_{\mathrm{T}}$	total mass of the system
m_0	mass of the spacecraft bus
n	number of serial rigid body links
$n = 0$	link representing the spacecraft body
$n+1$	payload link
n_i	moment on link i as a result of link $i-1$ supporting outboard links
$\boldsymbol{n} = (n_x n_y n_z)^{\mathrm{T}}$	normal vector perpendicular to the end-effector finger grip (tilt) for $i = n$
$N_{\mathrm{c}i}$	total moment about the link i centre of mass
N_{r}	total reaction torque about the centre of mass of the spacecraft bus with respect to the inertial coordinates
N_{T}	total moments acting at the manipulator base $(x_0 y_0 z_0)$ with respect to the base coordinates
N_0	total moments acting at the manipulator base $(x_0 y_0 z_0)$ with respect to the inertial coordinates
$p_{\mathrm{c}i}$	location of the centre of mass of link i with respect to the base coordinates
p_{i-1}	position of the link i origin with respect to the base coordinates
p^*	position of the end-effector with respect to the inertial coordinates
$p^*_{\mathrm{c}i}$	position of the link i centre of mass with respect to the inertial coordinates
p^*_{cm}	location of the centre of mass of the total robot/spacecraft system with respect to the inertial coordinates
$\boldsymbol{p} = (p_x p_y p_z)^{\mathrm{T}}$	Cartesian position vector of the end-effector with respect to the base coordinates
$\boldsymbol{P}$	linear momentum of the system
$\boldsymbol{q} = (\boldsymbol{nsap})^{\mathrm{T}}$	generalized Cartesian position of the end-effector with respect to the base coordinates

The MS was received on 19 March 2004 and was accepted after revision for publication on 25 April 2004.

$r_{ci} = (p_{ci} - p_{ci+1})$ distance between the centres of mass of adjacent links with respect to the base coordinates

r_{c0} position of the spacecraft centre of mass with respect to the inertial coordinates

$\dot{r}_i$ velocity of the centre of mass of each rigid body component of the system

$\boldsymbol{r}_i = (p_{I-1} - p_{ci})$ vectorial distance from the origin of link i to the centre of mass of link i

R_0 attitude of the spacecraft with respect to the inertial coordinates

$\boldsymbol{R}_i = (\boldsymbol{n}_i \boldsymbol{s}_i \boldsymbol{a}_i)$ 3×3 direction cosine matrix of each link with respect to the base coordinates

$\boldsymbol{s} = (s_x s_y s_z)^{\mathrm{T}} = \boldsymbol{a} \times \boldsymbol{n}$ slide vector parallel to the end-effector finger grip (twist) for $i = n$

$\boldsymbol{s}_i = (p_{ci} - p_i)$ vector position of the link i centre of mass from joint i

$\boldsymbol{s}_0$ position vector of the manipulator base with respect to the spacecraft body centre of mass

v_{ci} linear velocity of the link i centre of mass

v_i linear velocity of joint i

$\dot{v}_{ci}$ linear acceleration of the link i centre of mass

$\dot{v}_i$ linear acceleration of joint i

w_i angular velocity of joint i

$\dot{w}_i$ angular acceleration of joint i

W work done

$\boldsymbol{V}_i = (v_i w_i)^{\mathrm{T}}$ 6×1 velocity vector of joint i

z_{i-1} rotational axis of joint i

$\theta = (\theta_1 \ldots \theta_n)^{\mathrm{T}}$ joint angle displacements of each robotic link

$\tau = (\tau_1 \ldots \tau_n)^{\mathrm{T}}$ robot joint torques

1 INTRODUCTION

On-orbit servicing is a major application of space robotics with significant implications for increasing the availability of the current and future satellite fleet. This approach to space infrastructure development has significant commercial potential [**1**]. Space robotics generally is characterized by introducing significant problems concerning the control of manipulators in space—this is still a problem requiring an adequate solution (von Winnendael, 2002, personal communication). The primary differentiating characteristic of on-orbit servicing space robotics from terrestrial robotics is that the robot operates in a microgravity environment. The environmental disturbance torques (gravity gradient, solar pressure, aerodynamic and magnetic torques) imposed on the robot spacecraft are very low at $\sim 10^{-6}$ N m [**2**]—for the purposes of this paper, these can be ignored as negligible. Whereas a terrestrial robot is mounted onto terra firma, in space there is no such reaction force/torque cancellation to the motion of the robotic arms. The motions of the manipulators will generate reaction forces and moments on the spacecraft platform at the spacecraft mounting/manipulator coupling points. This will induce translational and rotational motion of the satellite platform in response to the movements of the manipulators. If no compensation is made for the motion of the mounting spacecraft, the robot end-effectors will not attain their targets since the coupling has a significant effect on the manipulator kinematics, dynamics and control. Feedforward thruster control may be utilized to compensate for the motion of the spacecraft mount, but this introduces undesirable and prohibitively excessive expenditure of fuel as fuel capacity is a major design driver to all spacecraft. Indeed, it has been found that fuel expenditure of space-based manipulators is prohibitive [**3**]. Furthermore, the fuel is required for orbit transfers which defines the redeployment capabilities of the on-orbit servicer. In addition, thrusters are difficult to control proportionally since they operate in pulse mode which introduces limit cycles. Hence, it is highly desirable to avoid the use of critically finite resources such as propellant.

2 REVIEW OF THE LITERATURE ON SPACE-BASED MANIPULATOR KINEMATICS AND DYNAMICS

Generalized multi-body dynamics in space has attracted interest for some years owing to its applicability to orbiting spacecraft which are characterized by complex, extended structures. A space-based manipulator system may be regarded as a multi-body system represented as a kinematic chain of interconnected rigid bodies (links). The first dynamics formulation for multiple bodies in space determined that, for n rigid bodies connected by rotational joints in an arbitrary open topological tree configuration (i.e. no closed loops), any rotational motion of the bodies produced a relative translation with respect to each other [**4**]. The notion of the connection barycentre was introduced which was defined as the composite centre of mass of each body from 0 to n obtained by loading each joint of the body with the total residual mass of the system connected to that joint; i.e. the mass distribution is represented by the total mass of inboard links acting on the inboard joint i and the total mass of outboard links acting on the outboard joint $i+1$ to form an augmented body. The connection barycentre for each link defined from the

system centre of mass is given by [4]

$$c_i = \sum_{j=0}^{i-1} \frac{m_j}{m_T} \boldsymbol{r}_i + \sum_{j=i+1}^{n} \frac{m_j}{m_T} \boldsymbol{s}_i \tag{1}$$

The barycentric concept was used to derive the inertia dyadics for the Newton–Euler dynamic equations to describe the attitude equations of the system. This technique was extended by eliminating the constraint torques for the n-body attitude equations using the Lagrangian method and so reducing the number of equations to be solved [5]. The direct path approach to multi-body dynamics involves determining the contribution of the motion of each body singly to coefficient matrices of the overall dynamic equations describing the system [6]. The direct path is a vectorial path from the main reference body 0 to each separate body j centre of mass comprising the system. The motion of each body influences the motion of the whole system. Since linear and angular positions, velocities and accelerations are related to the other bodies and to the reference coordinates kinematically, these direct path vectors transform the influence of the motion of one body to the other bodies. The direct path method has been adapted by introducing the concept of path matrices and reference matrices which describe the particular topology of the system [7]. Primitive equations of motion for each body were derived separately, considering them to be freebodies. By converting inertial velocities to relative velocities using linear operators, the constraints of motion were applied to the system equations. Hughes suggested that the direct path method is superior to the barycentric approach and is suited to implementation through Newton–Euler dynamic analysis [8]. The direct path method and the barycentric approach are closely related in that they both involve the construction of composite bodies. However, the method is unsuitable for closed-chain configurations whose inertial velocities cannot be expressed as independent sets of relative velocities for each body. These methods are very general and may be applied to multiple-degree-of-freedom joints as well as for forward dynamic analysis for simulation. However, generality is not an issue for space robotic control which only requires inverse dynamic solutions where each actuator has only a single degree of freedom which determines the relative motion between the links, and efficient dynamic equations have been developed for these problems. Robot dynamics is concerned with relating joint motions (position, velocity, acceleration) to the required joint torques to achieve those motions. The required actuator joint torques are computed to enforce tracking of the prescribed trajectory describing the Cartesian motion of the end-effector.

A number of research activities have considered the introduction of flexibility into multi-body dynamics, particularly associated with large, extended structures typical of space stations, and the problem of vibration suppression of flexural dynamics—the Space Station has a fundamental vibration frequency of resonance of $\sim$0.1 Hz which lies uncomfortably close to typical control cycle frequencies [9, 10]. The chief problem is that vibration inputs can cause the mounting spacecraft platform to tumble. Structural flexibility is also likely to be non-negligible in long boom-like manipulators which require damping by active control to behave more like rigid manipulators—this is typically achieved using a low-authority controller which damps out structural vibrations while a high-authority controller provides the nominal control effect assuming rigid bodies [11, 12]. There are two sources of flexibility in a boom-like manipulator. Elasticity may be incorporated as joint elasticity with finite rotational stiffness properties—a joint stiffness spring constant of 1–10 N m/rad would indicate a stiff joint, while values of 10^3–10^4 N m/rad characterize flexible joints which may be incorporated readily into Newtonian dynamic approaches. Flexibility may also be incorporated by modelling the rigid spacecraft body with flexible appendages as Euler–Bernoulli cantilever beams with flexural rigidity EI (but zero torsion). Energy-based Lagrangian techniques are most commonly used in which the strain energy of a single beam is modelled in the form

$$U = \frac{1}{2} EI \left(\frac{\partial^2 w}{\partial q^2} \right)^2 \mathrm{d}\boldsymbol{q}$$

where

$$w_{ij}(x,t) = \sum_{j=1}^{N} \phi_{ij}(x_i) q_{ij}(t)$$

and where

N = number of modes
ϕ_{ij} = eigenfunction of the cantilever beam
q_{ij} = modal coordinate

Normal rigid body robotic control systems can be readily adapted to modal control to suppress vibrations by using a 'virtual rigid manipulator' approach—this is achieved by replacing actual end-point kinematic variables with those of a 'virtual rigid manipulator' [13]. This approach, in spite of the increased degrees of freedom introduced by flexibility, allows the use of a smaller number of joint actuators to enforce tracking of the desired end-effector trajectory. Most flexible dynamic formulations require full state sensory observation of the system dynamic parameters which will not necessarily, or indeed typically, be the case. Therefore, flexibility is not considered further here other than to note that it is essential to ensure that the algorithm

control computation frequency is well separated from the resonant frequency responses of appendages such as solar panels, robotic manipulators and antennae. It is possible to preplan control inputs such that perturbations about the nominal trajectory owing to excitation of structural vibrations remain within bounds by specifying knot points of the trajectory to have zero acceleration or jerk [**14**].

In general, there are two main approaches to quantifying the dynamics of robot manipulators: the Lagrange–Euler (LE) technique [**15**] and the Newton–Euler (NE) technique [**16**] (excluding more exotic techniques such as characterizing robot dynamics as a Kalman filter problem through the introduction of spatial operators [**17**, **18**]), and these two formulations are in fact equivalent [**19**]. Both generate a set of six coupled second-order non-linear differential equations in position, velocity and acceleration. The LE technique yields highly structured equations highly suited to control analysis in state-space form, yielding the general form of the dynamics such that the joint torques for an n-link manipulator are given by [**20**]

$$\tau_i = \sum_{k=1}^{n} \mathbf{D}_{ik}(\theta)\ddot{\theta}_k + \sum_{k=1}^{n}\sum_{m=1}^{n} \boldsymbol{H}_{ikm}(\theta,\dot{\theta}) + \boldsymbol{G}_i(\theta) + \boldsymbol{B}_i\dot{\theta}_i + n\boldsymbol{K}_i(\theta_i - \delta_i) \quad (2)$$

where

$\mathbf{D}_{ik}(\theta) = n \times n$ mass inertia matrix

$\boldsymbol{H}_{ikm}(\theta,\dot{\theta}) = n \times 1$ vector of non-linear Coriolis and centrifugal forces

$\boldsymbol{G}_i(\theta) = n \times 1$ gravity loading vector

$\boldsymbol{B}_i = n \times 1$ actuator viscous damping coefficient (including dry Coulomb friction)

$\boldsymbol{K}_i = n \times 1$ actuator joint stiffness

$\delta_i =$ elastic joint deformation (for stiff joints, $\delta_i = \theta_i$)

$n =$ motor gear ratio

The advantage of the microgravity environment of space is that the joint torques are no longer required to support the gravitational loading of the manipulator and its payload [**21**]. It is also possible to cast the LE dynamics in end-effector (operational space) coordinates [**22**], but the computational complexity of this approach exceeds that of the LE formulation in the joint coordinates outlined above. The computational complexity of the LE method is polynomial with $O(n^4)$ such that the number of floating point computations (multiplies and additions) grows to the fourth power with the number of links n. For a space-based manipulator, this is a significant problem given the decade-long technological lag in space-rated computer processors.

The NE formulation of manipulator dynamics exploits d'Alembert's principle of virtual work by constraint forces which is applied to each link sequentially [**23**]. d'Alembert''s principle differentiates between inertial and virtual forces in which virtual forces act as constraints (but do not perform physical work) of the form $\mathrm{d}F - \ddot{R}\,\mathrm{d}m = 0$. This involves the forward propagation of generalized velocities and accelerations from the base of the manipulator to the end-effector—the velocity of each link is the sum of velocities of previous links and its own relative velocity. Then, the reverse propagation of generalized forces from the end-effector back to the base of the manipulator is computed. Unlike the LE method which eliminates constraint forces (unless Lagrange multipliers are used), the NE technique allows explicit computation of the constraint forces that are essential for robotic assembly tasks which introduce interaction forces with the environment. Furthermore, the recursive NE dynamic formulation is readily extensible to flexible systems through the spatial operator formalism [**24**]. The recursive NE method is extremely efficient, with a linear computational complexity of $O(n)$ and a significant improvement over LE approaches, particularly when $n \geqslant 3$, which applies to robotic manipulators required for on-orbit servicing [**25**]. A recursive formulation for the Lagrangian dynamics method was derived which reduced its complexity from $O(n^4)$ to $O(n)$ [**26**]. It was shown through tensor methods that the NE and LE recursive formulations were mathematically equivalent since the nine-element time derivative of the 3×3 rotational matrix of the LE formulation equates to the three-element angular velocity components of the NE formulation [**19**]. However, the NE method remains 60 per cent more efficient than the recursive LE method, and for this reason was adopted for dynamic simulation of all Canadian space manipulators. Several dynamic formulations for multi-body space systems have been subject to comparison, and these analyses conclude that recursive NE methods are much more efficient computationally than LE approaches [**27**], a conclusion reiterated in its application to space-based manipulators [**28**]. A derivative method of the NE technique—Kane's equations—numerically linearizes the kinematics to give generalized velocities and enables the derivation of generalized forces by serial approximation [**27**]. These equations were adapted specifically for robotics applications [**29**] which formed the basis of an approach to the analysis of a two-armed space robot [**30**]. This approach exploited the purely closed-chain kinematic configuration without considering the contact interaction forces of the end-effectors.

For the dynamics of a robotic on-orbit servicer with manipulators, there is a fairly specific multi-body configuration, with the positioning of the end-effector of a manipulator(s) to a target in Cartesian space being of specific concern. This places a premium on under-

standing the relative configuration of each link of the multi-body system with a view to controlling that configuration in order to position the end-effectors correctly to perform on-orbit servicing tasks on a target spacecraft. For instance, a six-degree-of-freedom manipulator mounted onto a six-degree-of-freedom spacecraft platform generates a twelve-degree-of-freedom system controlled by only six motor joint inputs, assuming that there is no independent attitude actuation. The system is redundant since both vehicle and manipulator have more controllable states than are necessary to specify the motion of the end-effector (this is characterized by a non-square Jacobian matrix). The kinematics and dynamics do not generate closed-form solutions for generalized position owing to their inherent redundancy. This form of generalized position control of a satellite mounted with a three-degree-of-freedom manipulator was found to have an infinite number of solutions to the inverse kinematics due to this redundancy [**31**]. The solutions are a function of the history of manipulator motion rather than joint angle configuration alone. Solutions can be obtained but usually involve the introduction of selective cyclic 'coning' motions superimposed on the desired manipulator trajectory to maintain constant spacecraft attitude without employing dedicated attitude control actuators [**31**–**34**]. Reorientation of spacecraft attitude using such coning motions requires that the dynamic parameters be well known, but the inertias and masses of the system will be subject to change owing to unknown payloads. In addition, propellant usage throughout the mission results in variable inertia properties of the servicer platform. Such coning motions may introduce possible collision hazards with target satellite appendages which would require complex path planning to avoid, and maintenance of stabilized attitude is essential for similar reasons. Overcoming these issues by using small cyclic motions to eliminate non-negligible non-linear terms introduces the requirement for many cycles for even small changes in spacecraft attitude. The virtual manipulator approach may be used to derive the conservation of angular momentum in relative joint coordinates [**32**, **33**]. Only the end-effector trajectory was controlled while the satellite attitude was allowed to be arbitrary. Clearly this is not desirable since the spacecraft bus will have components and subsystems that have their own specific pointing requirements. Another formulation is to find the generalized Jacobian matrix $\mathbf{J}^*$ by applying applied momentum constraints to a complete freefloating spacecraft/manipulator to account for platform translation and rotation by relating end-effector velocities to joint and platform velocities [**35**–**38**]. Such freefloating systems are defined by their lack of a dedicated spacecraft attitude control system. The generalized Jacobian, owing to its dynamic nature, is complex to compute with a complexity of $O(n^2)$ and so not conducive to real-time operation onboard space-rated processors [**39**]. A dynamic coupling coefficient may be defined to quantify the relation between the end-effector velocity and base velocity [**40**]

$$\begin{pmatrix} v_0 \\ w_0 \end{pmatrix} = \boldsymbol{P} \begin{pmatrix} v_n \\ w_n \end{pmatrix} \tag{3}$$

This dynamic factor $\boldsymbol{P}$ is similar to the generalized Jacobian and may be reduced to a single value, $C = \det(\boldsymbol{P}^{\mathrm{T}}\boldsymbol{P})$ to quantify the coupling effect. The Japanese ETS (Engineering Test Satellite) VII spacecraft (1998), which sported a 2 m long six-degree-of-freedom manipulator, tested many of the technologies required for rendezvous, docking and on-orbit servicing and found that the dynamic coupling between the manipulator and the spacecraft base imposed significant control difficulties [**41**]. ETS VII comprised two satellites, a 2.5 t chaser spacecraft with a 0.15 t six-degree-of-freedom manipulator and a 0.4 t target spacecraft. Evidently, dedicated attitude control would reduce this coupling effect by making $w_0 = 0$. However, this was only an analytical factor to characterize the coupling rather than having any application for control purposes. The generalized Jacobian comprises the conventional Jacobian of computational complexity $O(n)$ with additional terms dependent on the masses, inertias and geometric structures of each link which generate the additional complexity [**39**]. The conventional Jacobian could be used to derive a transposed Jacobian which yielded satisfactory results when the platform–manipulator mass ratios were in excess of ~ 5. This, however, limits the applicability of the formulation where it is conceivable that freeflyer robotic systems will have mass ratios (particularly owing to large payloads) significantly less than this.

It has been found that freefloating systems are subject to unpredictable dynamic singularities in their manipulator workspaces owing to the attitude motion of the platform at which point they become unstable [**42**, **43**]. Kinematic singularity occurs in terrestrial manipulators when two or more axes align, resulting in the loss of one or more degrees of freedom, i.e. when the determinant of the Jacobian matrix becomes zero: $|\mathbf{J}(\theta)| = 0$. For a spacecraft-mounted manipulator, singularities are no longer purely kinematic. Dynamic singularities are a function of both robotic kinematics and the dynamic properties of both the manipulator and the spacecraft. Spacecraft attitude is a function of path history owing to its non-holonomic nature (defined later). If spacecraft attitude is not controlled, the 'path independent workspace' reachable by the manipulator is much smaller than the 'constrained workspace' available to the manipulator mounted onto a spacecraft employing attitude control. Dynamic singularities are characteristic of the 'path dependent workspace' (which is much larger than the path independent workspace) reachable by a manipulator mounted onto a non-attitude-controlled

spacecraft. Indeed, dynamic singularities are characteristic of freefloating systems and are functions of the mass and inertia of the composite spacecraft/manipulator system. These singular joint configurations cannot be mapped into unique points in the workspace since the generalized Jacobian is a dynamic function rather than being purely kinematic, and spacecraft attitude coordinates do not map uniquely to end-effector coordinates. Hence, these singularities cannot be predicted from the kinematic configuration alone since they are also functions of the history of the end-effector path; i.e. points in a workspace may become singular depending on the path taken to reach them. The path independent workspace, however, does not suffer from dynamic singularities and has its maximum extent when attitude control is employed, i.e. when it coincides with the constrained workspace. Any control system that uses inverse generalized Jacobian techniques for freefloating systems will encounter such singularities within the workspace. Although the bidirectional approach attempts to alleviate this problem of free-floating systems, this method is computationally intensive since the scheme relegates the problem to the path planning algorithms higher up the control hierarchy by using the extra degrees of freedom for path planning [**44**]. The bidirectional search mapped between the original state and final desired configuration using the generalized Jacobian to avoid excessive joint torques, for obstacle avoidance or for reorientation of attitude. A Moore–Penrose pseudo-inverse version of the generalized Jacobian $(\mathbf{J}^*)^+ = \mathbf{J}^{*\mathrm{T}}(\mathbf{J}^*\mathbf{J}^{*\mathrm{T}})^{-1}$ was used to overcome the dynamic singularities problem by using the redundant degrees of freedom [**45**]. It allowed changes in spacecraft attitude while keeping the generalized position of the end-effector fixed with respect to the inertial reference frame to provide greater flexibility of operation. However, this formulation is even more complex than the generalized Jacobian technique. Excessive spacecraft motions may occur which cannot be accounted for in path planning, so standard robotic minimum-time optimal trajectory generation may be used to limit joint torques and attitude rates to within specified bounds [**46**]. Control schemes have been devised that switch between different coordinated modes of control. This involves control of the platform/manipulator being switched from the freefloating formulation to a redundancy formulation for the control of the platform alone whenever dynamic singularites are encountered [**42**, **43**, **47**]. However, switching is characteristic of variable-structure control schemes and these tend to suffer from 'chattering' induced by rapid switching. This can excite high-frequency dynamic responses and is clearly undesirable for a space-borne manipulator which operates in an undamped medium, but a saturation function as used in sliding control can be used in place of a switching function [**48**]. In conclusion, then, freefloating systems are subject to certain constraints not encountered in terrestrial robotics [**49**]:

1. Spacecraft orientation is required to derive the generalized Jacobian.
2. Dynamic properties affect the kinematics.
3. Dynamic singularities occur in the workspace.
4. Non-holonomic redundancy implies path dependency of joint angle configuration.

All such schemes which leave spacecraft attitude uncontrolled cannot cope with the input dynamics of target acquisition in real time using present-day and near-future space-rated computational hardware. The alternative is to employ dedicated attitude actuation—the fact that attitude control is specifically employed on all spacecraft to date suggests the validity of this approach. A single arm mounted onto a space robot system with orthogonal reaction wheels for attitude control has 15 degrees of freedom [**50**, **51**]. Such a system comprises a nine-degree-of-freedom invertible portion including manipulator joint angles and base orientation and a six-degree-of-freedom component including the base position and reaction wheel positions. In this analysis, the reaction wheel dynamics was incorporated to eliminate reaction wheel position, and base translation was eliminated by application of the conservation of linear momentum. By globalizing the dynamics and control of the whole system, the inherent computational advantages of utilizing such a distributed set of actuations was lost. A similar problem to the free-floating spacecraft mounting a number of simple manipulators has been analysed in reference [**52**]. The primary purpose of this analysis was to generate attitude stabilization of the spacecraft using a distributed set of reaction wheels and manipulator arms through 'shape control'. Each manipulator joint was treated dynamically as a reaction wheel, and each manipulator was restricted to a maximum of three degrees of freedom to provide three-axis attitude stabilization (depending on the number of reaction wheels employed). Shape control was defined as the manipulator joint configuration required to control attitude—it bears strong similarities to the coning approach outlined above in exploiting the redundancy in the system dynamics. However, the present concern is with the specific use of manipulators to perform useful manipulation functions rather than merely attitude stabilization. Emphasis is on the development of manipulator control in Cartesian space for the purpose of on-orbit servicing tasks. The employment of simple manipulators for the purpose of pure spacecraft attitude control is unlikely given the current approaches to attitude control and the mechanical complexity overhead of mounting manipulators onto spacecraft unless they serve a specific and unique function (such as for manipulation tasks).

Longman *et al.* have applied classical NE dynamics techniques to the remote manipulator servicer (RMS)

mounted onto the Space Shuttle [53, 54]. They used two models of the manipulator: one with a prismatic elbow joint and one with a revolute elbow joint. This marked the first detailed analysis of the space robotics problem in a practical sense. They decoupled the translation and rotation components of the combined RMS/Shuttle system and calculated the total reaction moment on the Space Shuttle owing to the motion of the RMS. Although the mass of the RMS is much smaller than the mass of the Space Shuttle (of 90 t), it is rated for large cargo-handling payloads of up to 30 t. Hence, the payloads to be handled by a robotic on-orbit servicer will not be insignificant fractions of the servicer system mass. During RMS operation, it is controlled by the onboard teleoperator, and the Shuttle reaction control system (RCS) which provides attitude control is switched off. These formulations were manipulator geometry specific rather than generalized as presented here.

Some workers have considered two-arm systems since these offer more realistic models of future robotic systems. The generalized Jacobian approach may be extended to consider dual-arm coordination while mounted onto a space platform [55]. This generalized Jacobian was a composite 18×18 element matrix even larger than the original 6×6 generalized Jacobian required for a single arm. To provide coordinated control, it was suggested that, while one arm was used for task operations, the other arm should be moved in compensatory mode to keep the satellite attitude stable and minimize the total torques applied to the spacecraft mount. Quite apart from the excessive computational overhead of inverting a 18×18 Jacobian matrix at each control cycle, the use of a manipulator as a dedicated attitude stabilizer is wasteful of costly hardware since it effectively reduces (operationally speaking) the dual-arm system to a single-arm system as well as imposing possible collision problems. The appropriateness of two arms derives from its operational capabilities. A two-armed robot mounted onto a satellite platform was considered in reference [56] for which a set of closed-form Newton–Euler equations for both manipulators was derived. Once again, their formulation involved an 18×18 Jacobian transpose matrix precluding the formulation from real-time operation. A number of suggestions have been made to simplify the computations for such space-based manipulator control, including assuming that the angular momentum is dominated by the end-effector, wrist and payload [57].

Many of these approaches are computationally demanding, particularly those associated with the generalized Jacobian, and do not consider the limited computational resources available within spacecraft. It is suggested that a piecewise approach to the problem is more suitable for a distributed implementation through a dedicated attitude control system for the spacecraft and a separate robot control system. The present concern is to simplify the computations, allow a distributed approach by employing dedicated attitude control (a mature spacecraft technology) and exploit heritage from pre-existing robotic control algorithms such as the Robot Control C Library (RCCL). Dynamic analysis algorithms should have the following desired properties [58, 59]:

(a) versatility,
(b) adaptability,
(c) reliability,
(d) computational efficiency,
(e) user friendliness.

Most dynamic analysis approaches possess the first three properties but computational efficiency is essential for real-time control implementation, and user friendliness is essential for transparency and inheritability. It is these last two considerations that are essential for space application—the 'engineering approach' (as opposed to a mathematically aesthetic approach) presented here is explicitly pragmatic and achievable within these constraints.

3 FREEFLYING ROBOTIC KINEMATIC-DYNAMIC PROBLEM FORMULATION

The robotic freeflyer spacecraft system under consideration here comprises a spacecraft bus mount and one or more robotic manipulators. The introduction of manipulators into space creates a major problem as the kinematic and dynamic analysis requires the definition of reference frames—firstly, a base reference frame and then subsequent reference frames whose origins coincide with each robotic joint. For a six-degree-of-freedom robotic manipulator, this means six reference frames. For a terrestrial robot, the base reference frame is the point at which the robot is grounded—this is the inertial reference frame of world coordinates. In space, of course, this inertial reference frame no longer exists—any motion of the manipulators generates a reaction effect on the robot mounting platform which is free to move, so the base reference frame moves and cannot be considered an inertial frame of reference. The emplacement of relative coordinate frames of the space-based robotic system is no longer described by purely kinematic considerations as in a terrestrial manipulator but must be described in terms of combined kinematic and dynamic properties. The manipulator configuration is determined by its kinematic structure but also requires inclusion of the inertial properties of the system. An inertial reference frame from which the external world can be described must thus be defined alternatively [60]. This problem was for a number of years considered to be one of the major stumbling blocks in the development of robotic freeflyer servicers. There have been other

solutions proposed such as the generalized Jacobian for resolved rate control, but this imposes prohibitive computational requirements far in excess of the computational processing speeds achievable by space-rated hardware [**32**]. Most research into this problem has concentrated on further developments of the generalized Jacobian to ever more fanciful control laws that cannot be readily implemented on space-rated hardware. Furthermore, there are severe disadvantages of such methods which are outlined in the previous section and the conclusions [**36**–**38**]. It has been suggested that spacecraft attitude might be maintained by generating coning motions of the robotic manipulators (analagous to the use of spinning wheels), but such an approach presents problems for collision avoidance with on-orbit target satellites which are generally complex and extended in shape [**31**, **34**].

There are two possible reference frames that may be used: an inertial reference frame fixed at the centre of the Earth, and an orbital reference frame whose origin lies at the orbit altitude, or the system reference frame with its origin at the system centre of mass. The geocentric reference frame is unnecessary as the motions of the robotic spacecraft are much smaller than the characteristic distance to the centre of the Earth. The orbital reference frame is in fact defined by the system centre of mass which moves in orbit around the Earth and may be represented by classical Keplerian elements

$$R_{\mathrm{cm}} = \frac{H^2}{GM_{\mathrm{E}}(1 + \epsilon \cos\theta)}$$

where

$R_{\mathrm{cm}} = R_{\mathrm{E}} + h$,
$R_{\mathrm{E}} =$ radius of the Earth
$h =$ orbital altitude
$H =$ angular momentum
$G =$ universal gravitation constant
$M_{\mathrm{E}} =$ mass of the Earth
$\epsilon =$ orbital eccentricity
$\theta =$ orbital true anomaly

The orbit is similarly much larger than the local motions of the robotic spacecraft. The system centre of mass is thus adopted as the inertial reference frame [**61**]. Initially, an arbitrary robotic spacecraft is considered with a single manipulator arm composed of n manipulator links, plus a rigid body spacecraft mounting platform (referred to as rigid body $i = 0$). Each rigid body is referred to as a rigid link and the formulation is readily generalized to deal with m manipulators. The origin of each link represents the origin of each consecutive reference frame propagated from the base of the robotic manipulator out to the end-effector of the manipulator. The total system is treated as a kinematic chain (multiple robot arms may be treated as branched kinematic chains). The linear momentum conservation law states that the total linear momentum of the system is conserved

$$\boldsymbol{P} = \sum_{i=0}^{n+1} m_i \dot{\boldsymbol{r}}_i = \text{constant} = 0 \tag{4}$$

This is arbitrarily true since

$$\dot{\boldsymbol{P}} = \sum_{i=0}^{n+1} \boldsymbol{F}_{ext} = 0$$

As a holomonic constraint, this is integrable to the equilibrium of moments principle

$$\int_0^t \sum_{i=0}^{n+1} m_i \dot{\boldsymbol{r}}_i \, \mathrm{d}t = \left[\sum_{i=0}^{n+1} m_i \boldsymbol{r}_i \right]_0^t = 0 \tag{5}$$

Similarly, angular momentum conservation states that

$$\boldsymbol{L} = \sum_{i=0}^{n+1} \mathbf{I}_i w_i + m_i \dot{\boldsymbol{r}}_i \times \boldsymbol{r}_i = \text{constant} = 0 \tag{6}$$

This is arbitrarily true since

$$\dot{\boldsymbol{L}} = \sum_{i=0}^{n+1} \boldsymbol{N}_{\mathrm{ext}} + \sum_{i=0}^{n+1} \boldsymbol{r} \times \boldsymbol{F}_{\mathrm{ext}} = 0$$

As a non-holonomic constraint, this is not integrable—integration of rotational velocity does not yield a unique vectorial representation of orientation since rotational motion is path dependent owing to the non-commutativity of rotations. There are thus an infinite number of paths yielding a particular orientation; i.e. orientation depends on the time history of motion [**44**]. This derives from the definition of holonomy [**39**]:

> A system is holonomic if and only if its motion is constrained by a set of algebraic equations involving only general angular coordinates and time. This implies that a system is holonomic if and only if a set of vector fields defining the linear space of possible velocities is completely integrable everywhere in general coordinates. Otherwise, it is nonholonomic.

Hence, in this case there are more controllable states than are necessary to specify the motion of the end-effector.

Most of the formulations in section 2 treat the linear and angular aspects of the space-based manipulator problem together in a unified framework that is readily cast into LE form which, although attractive from a mathematical viewpoint, suffers from $O(n^4)$ complexity compared with the NE formulation which has $O(n)$ complexity [**23**]. Such a unified treatment of linear and angular momentum/energy does not correlate well with the nature of spacecraft design. Spacecraft generally

employ dedicated orbit control systems (i.e. orbit maneouvring thrusters) and dedicated attitude control systems (be they thrusters, wheels or control moment gyroscopes) which are controlled separately. A dedicated attitude control system is essential for any spacecraft that has pointing requirements. As the spacecraft engineering implementation separates the orbit and attitude control hardware, so the control should also be separate. This considerably eases the computational burden of coping with non-holonomy.

By decoupling the system such that linear and angular motions are treated separately, real-time control is possible and straightforward by considerably reducing the complexity of the problem. The translation effects are holonomic constraints as outlined above, so linear momentum constraints may be integrated and be applied to the system through the equilibrium of moments. This accounts for the translational motion of the satellite in inertial space. The system centre of mass remains invariant in inertial space, providing unique closed-form solutions for translation motion control by incorporating linear compensation into the robot kinematics formulation. These translational kinematic equations have the same form as those for a terrestrial manipulator. Hence, the linear component of the reaction effect is compensated for automatically within the linear portion of the controller without the use of fuel.

The angular effects are non-holonomic constraints since the attitude of the platform and the orientation of the end-effector depends on the history of joint displacements owing to the non-commutativity of finite rotation sequences. Different trajectories of the manipulator can end in the same orientation of the end-effector but will result in different attitudes for the spacecraft. Hence, angular momentum conservation constraints are not integrable to unique values of spacecraft attitude as a function of manipulator joint angles. Angular momentum conservation constraints must be applied directly. It is possible to do this straightforwardly by employing active three-axis attitude stabilization by non-fuel expending wheels—momentum wheels (MWs), reaction wheels (RWs) or control moment gyroscopes (CMGs) [**62**]—to compensate for the dynamic attitude reactions based on computations of the reaction forces and moments applied at the base of the robotic manipulators. Such spinning wheels effectively redistribute angular momentum within the spacecraft. Computer simulations presented later suggest that reaction wheels and momentum wheels cannot produce sufficient torque to compensate for the reaction effects of the motion of the robot arms [**63**]. The reaction forces and torques acting on the spacecraft mounting owing to the manipulators may be calculated directly from the manipulator dynamics and be fed forward to the attitude control system. The CMGs are then driven to counteract the reaction forces and moments on the spacecraft mounting in conjunction with standard attitude error control algorithms to maintain spacecraft attitude. This method allows the end-effector position and orientation to be formulated as a unique function of joint angles independent of the end-effector path.

4 SPACE-BASED KINEMATICS SOLUTION

For a freeflying robotic manipulator employing dedicated attitude control of the spacecraft bus, the position kinematics of a space manipulator with respect to inertial space may be represented by (see Fig. 1)

$$p^* = r_{c0} + R_0 s_0 + \sum_{i=1}^{n} \mathbf{R}_i \boldsymbol{l}_i \tag{7}$$

For an attitude controlled platform, $\mathbf{R}_0 = \mathbf{I}_3$. The centre of mass of the complete system (including the satellite bus mount, robotic manipulator and the payload) is given by the equilibrium of moments [**53**, **54**]

$$\left(\sum_{i=0}^{n+1} m_i\right) p^*_{\mathrm{cm}} = \sum_{i=0}^{n+1} m_i p^*_{ci} \tag{8}$$

Hence

$$p^*_{\mathrm{cm}} = \frac{\sum_{i=0}^{n+1} m_i p^*_{ci}}{\sum_{i=0}^{n+1} m_i} \tag{9}$$

It is necessary to find the location of the system centre of mass with respect to inertial coordinates where it remains invariant [**54**]. The location of the centre of mass will remain invariant in inertial space if no external forces act on the system

$$\sum_{i=0}^{n+1} F_i = \sum^{n+1} m_i \ddot{p}^*_{ci} = 0 \qquad \text{such that } \ddot{p}^*_{\mathrm{cm}} = 0 \tag{10}$$

This point corresponds to the 'virtual ground' defined

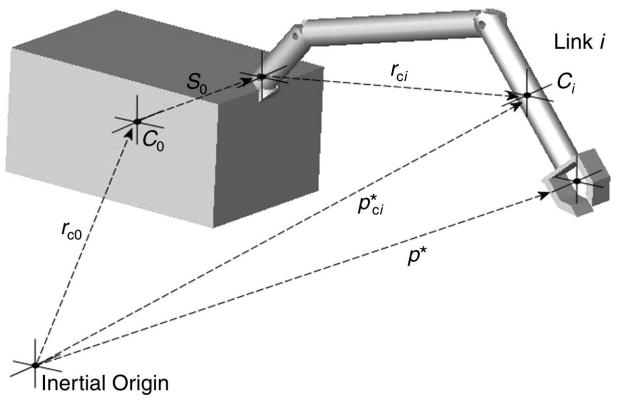

Fig. 1 Space freeflyer geometry

by the virtual manipulator approach—the inertial 'ground' of an ideal kinematic chain [**32**, **33**]. The virtual ground is the point in inertial space at which an ideal virtual kinematic chain manipulator has its base when its end-effector coincides with the end-effector of the actual manipulator. This virtual ground point coincides with the centre of mass of the spacecraft–manipulator system. This is to be expected since the constraints applied were the equilibrium of moments for the derivation of the kinematics of the virtual manipulator. The system centre of mass is the point at which all the mass may be considered to be concentrated (there is no corresponding centre of inertia).

Now,

$$p^*_{ci} = \sum_{j=0}^{i} \boldsymbol{r}_{cj}$$

Substitution into equation (9) yields

$$\begin{aligned} p^*_{cm} &= \frac{1}{m_T}\left(\sum_{i=0}^{n+1} m_i \sum_{j=0}^{i} \boldsymbol{r}_{cj}\right) = \frac{1}{m_T}\left(\sum_{i=0}^{n+1}\sum_{j=i}^{n+1} m_j \boldsymbol{r}_{ci}\right) \\ &= r_{c0} + \frac{1}{m_T}\sum_{i=1}^{n+1}\sum_{j=i}^{n+1} m_j \boldsymbol{r}_{ci} \end{aligned} \tag{11}$$

Now, the vector to the centre of mass of each link and the vectorial length of each link are defined as

$$\begin{aligned} \boldsymbol{r}_{ci} &= \mathbf{R}_i \boldsymbol{r}_i + \mathbf{R}_{i-1}\boldsymbol{s}_{i-1} \\ \boldsymbol{l}_i &= \boldsymbol{r}_i + \boldsymbol{s}_i \end{aligned} \tag{12}$$

These definitions are substituted into equation (11)

$$p^*_{cm} = r_{c0} + \frac{1}{m_T}\sum_{i=1}^{n+1}\sum_{j=i}^{n+1} m_j(\mathbf{R}_i \boldsymbol{r}_i + \mathbf{R}_{i-1}\boldsymbol{s}_{i-1})$$

The following manipulations attempt to restructure these equations to match terrestrial manipulator algorithms of the form: $p_i = \mathbf{R}_i \boldsymbol{l}_i$

$$\begin{aligned} p^*_{cm} &= r_{c0} + \frac{1}{m_T}\sum_{i=1}^{n+1}\sum_{j=i}^{n+1} m_j \mathbf{R}_{i-1}(\boldsymbol{r}_{i-1} + \boldsymbol{s}_{i-1}) \\ &\quad + \frac{1}{m_T}\sum_{i=1}^{n+1} m \mathbf{R}_i \boldsymbol{r}_i \\ &= r_{c0} + \frac{1}{m_T}\sum_{i=1}^{n+1}\sum_{j=i}^{n+1} m_j \mathbf{R}_{i-1}\boldsymbol{l}_{i-1} + \frac{1}{m_T}\sum_{i=1}^{n+1} m \mathbf{R}_i \boldsymbol{r}_i \end{aligned}$$

The components of the equation that do not correspond directly to the terrestrial manipulator kinematics (such as the spacecraft defined as body 0 and the payload defined as body $n+1$) are separated out

$$\begin{aligned} p^*_{cm} &= r_{c0} + \frac{1}{m_T}\sum_{i=2}^{n+1}\sum_{j=i}^{n+1} m_j \mathbf{R}_{i-1}\boldsymbol{l}_{i-1} \\ &\quad + \frac{1}{m_T}\left[\sum_{i=1}^{n+1} m_i \boldsymbol{l}_0 + \sum_{i=1}^{n+1} m_i \mathbf{R}_i \boldsymbol{r}_i\right] \\ &= r_{c0} + \frac{1}{m_T}\sum_{i=1}^{n+1} m_i \boldsymbol{s}_0 + \frac{1}{m_T}\sum_{i=1}^{n}\sum_{j=i+1}^{n+1} m_j \mathbf{R}_i \boldsymbol{l}_i \\ &\quad + \frac{1}{m_T}\sum_{i=1}^{n} m_i \mathbf{R}_i \boldsymbol{r}_i + \frac{m_{n+1}}{m_T}\mathbf{R}_{n+1}\boldsymbol{r}_{n+1} \\ &= r_{c0} + \left(1 - \frac{m_0}{m_T}\right)\boldsymbol{s}_0 + \frac{1}{m_T}\sum_{i=1}^{n} \mathbf{R}_i \\ &\quad \left(\sum_{j=i+1}^{n+1} m_j \boldsymbol{l}_i + m_i r_i\right) + \frac{m_{n+1}}{m_T}\mathbf{R}_{n+1}\boldsymbol{r}_{n+1} \end{aligned}$$

The equation has been separated out into three components: components associated with body 0 (the spacecraft), bodies 1 to n (the manipulator links) and body $n+1$ (the payload).

This reduces to

$$p^*_{cm} = r_{c0} + \left(1 - \frac{m_0}{m_T}\right)\boldsymbol{s}_0 + \sum_{i=1}^{n} \mathbf{R}_i \boldsymbol{L}_i + \left(\frac{m_{n+1}}{m_T}\right)\boldsymbol{r}_{n+1} \tag{13}$$

where

$$\boldsymbol{L}_i = \frac{1}{m_T}\sum_{j=i+1}^{n+1}(m_j \boldsymbol{l}_i + m_i \boldsymbol{r}_i)$$

This completes the location of the centre of mass of the system with respect to inertial space. It is assumed arbitrarily that the local inertial reference frame initially coincides with the satellite bus centre of mass, i.e. $r_{c0} = 0$, since any point fixed in the interceptor body may be regarded as inertially fixed prior to any robotic maneouvre. That point will remain fixed in inertial space as long as the task execution time is short compared with the orbital period of the satellite and it may be regarded as an inertial reference for any particular payload of mass m_{n+1}. This choice of inertial coordinates is not strictly inertial (as indeed no truly inertial reference frame exists within the universe) since it moves along the orbital trajectory with the spacecraft at the orbital velocity which causes a slow change in attitude pitch angle of the spacecraft as it orbits the Earth, typically $\sim 10^{-3}$ rad/s. However, given that this change in pitch attitude is much slower than local spacecraft attitude manoeuvres, this pitch variation is decoupled from the local spacecraft attitude which is defined from the local nadir direction to the centre of the Earth [**64**]. The local frame of reference defined by the system centre

of mass is thus sufficiently inertial such that spin angular momentum and orbital angular momentum are decoupled and may be considered independently [**61**]. This is similar to the assumptions used for relative phasing orbits defined by the Clohessy–Wiltshire equations (see the Appendix) [**65**]. The system centre of mass will then remain fixed in this local inertial space.

To continue the present generalized formulation, r_{c0} is substituted into equation (7) having defined p^*_{cm}

$$p^* = p^*_{cm} + \boldsymbol{s}_0 + \sum_{i=1}^{n} \mathbf{R}_i \boldsymbol{l}_i - \frac{1}{m_T} \sum_{i=1}^{n+1} \sum_{j=i}^{n+1} m_j \boldsymbol{r}_{ci} \tag{14}$$

Now, a similar procedure is followed to that employed for locating the centre of mass by defining the vector to the centre of mass of each link and the vectorial length of each link

$$\boldsymbol{r}_{ci} = \mathbf{R}_i \boldsymbol{r}_i + \mathbf{R}_{i-1} \boldsymbol{s}_{i-1}$$
$$\boldsymbol{l}_i = \boldsymbol{r}_i + \boldsymbol{s}_i$$

This is substituted into equation (14)

$$p^* = p^*_{cm} + \boldsymbol{s}_0 + \sum_{i=1}^{n} \mathbf{R}_i \boldsymbol{l}_i - \frac{1}{m_T} \sum_{i=1}^{n+1} \sum_{j=i}^{n+1} m_j (\mathbf{R}_i \boldsymbol{r}_i + \mathbf{R}_{i-1} \boldsymbol{s}_{i-1})$$

Again, an attempt is made to separate out the components relating to the spacecraft mounting (body 0), the manipulator links (bodies 1 to n) and the payload (body $n+1$)

$$\begin{aligned} p^* &= p^*_{cm} + \boldsymbol{s}_0 + \sum_{i=1}^{n} \mathbf{R}_i \boldsymbol{l}_i - \frac{1}{m_T} \left[\sum_{i=1}^{n+1} \sum_{j=i}^{n+1} m_j (\mathbf{R}_{i-1} \boldsymbol{r}_{i-1} + \mathbf{R}_{i-1} \boldsymbol{s}_{i-1}) + \sum_{i=1}^{n+1} m_i \mathbf{R}_i \boldsymbol{r}_i \right] \\ &= p^*_{cm} + \boldsymbol{s}_0 + \sum_{i=1}^{n} \mathbf{R}_i \boldsymbol{l}_i - \frac{1}{m_T} \left[\sum_{i=2}^{n+1} \sum_{j=i}^{n+1} m_j \mathbf{R}_{i-1} (\boldsymbol{r}_{i-1} + \boldsymbol{s}_{i-1}) \right] - \frac{1}{m_T} \left[\sum_{i=1}^{n+1} m_i \mathbf{R}_0 (\boldsymbol{r}_0 + \boldsymbol{s}_0) + \sum_{i=1}^{n+1} m_i \mathbf{R}_i \boldsymbol{r}_i \right] \end{aligned}$$

It is possible to begin to separate out and cluster the contributions from the spacecraft, the manipulator and the payload

$$\begin{aligned} p^* &= p^*_{cm} + \frac{m_0}{m_T} \boldsymbol{s}_0 + \sum_{i=1}^{n} \mathbf{R}_i \boldsymbol{l}_i - \frac{1}{m_T} \left[\sum_{i=1}^{n+1} \sum_{j=i+1}^{n+1} m_j \mathbf{R}_i (\boldsymbol{r}_i + \boldsymbol{s}_i) + \sum_{i=1}^{n+1} m_i \mathbf{R}_i \boldsymbol{r}_i \right] \\ &= p^*_{cm} + \frac{m_0}{m_T} \boldsymbol{s}_0 + \sum_{i=1}^{n} \mathbf{R}_i \boldsymbol{l}_i - \frac{1}{m_T} \left[\sum_{i=1}^{n} \sum_{j=i+1}^{n+1} m_j \mathbf{R}_i \boldsymbol{l}_i + \sum_{i=1}^{n} m_i \mathbf{R}_i \boldsymbol{r}_i \right] - \left(\frac{m_{n+1}}{m_T} \mathbf{R}_{n+1} \boldsymbol{r}_{n+1} \right) \end{aligned}$$

This gives the inertial position of the end-effector

$$p^* = p^*_{cm} + \frac{m_0}{m_T} \boldsymbol{s}_0 + \frac{1}{m_T} \sum_{i=1}^{n} \left(\sum_{j=0}^{i} m_j \boldsymbol{l}_i - m_i \boldsymbol{r}_i \right) \mathbf{R}_i - \frac{m_{n+1}}{m_T} \mathbf{R}_{n+1} \boldsymbol{r}_{n+1}$$

More succinctly

$$\begin{aligned} p^* &= p^*_{cm} + \frac{m_0}{m_T} \boldsymbol{s}_0 + \sum_{i=1}^{n} \mathbf{R}_i \lambda_i - \frac{m_{n+1}}{m_T} \mathbf{R}_{n+1} \boldsymbol{r}_{n+1} \\ \text{where } \lambda_i &= \frac{1}{m_T} \sum_{j=0}^{i} (m_j \boldsymbol{l}_i - m_i \boldsymbol{r}_i) \end{aligned} \tag{15}$$

Here, λ_i is defined as a lumped kinematic parameter for each mamipulator link.

5 RESOLVED MOTION CONTROL

The kinematics of robotic manipulators are defined such that at each joint i a reference frame is assigned to form a sequence of coordinate frames from the base (joint $i=0$) to the end-effector (joint $i=n$). There are two main approaches to kinematic description of robotic manipulators. Chasles' screw theorem describes the six-degree-of-freedom displacement of a body as a translation along a unique axis with a rotation about that axis. In this way, this approach bears some similarities to the theory of quaternions used for rotational kinematics. Neither of these formulations is used extensively in spacecraft attitude or robotic manipulator operational software, although both offer advantages in avoiding the incidence of singularities. The Denavit–Hartenberg (DH) 4×4 matrix formulation for robotic kinematics is well developed and widely used in robotics [**15**, **16**, **66**], while Lie groups are not [**67**]. The DH matrix relates each sequential coordinate frame from the base ($i = 0$) to the end-effector ($i = n$) to provide the basis for relating joint angles to the Cartesian position of the end-effector as a sequence of rigid body movements. The DH matrix formulation expresses the geometry of a space manipulator as a non-linear mapping given by [**63**, **68**]

$$\boldsymbol{q} = \begin{pmatrix} n & s & a & p^* \\ 0 & 0 & 0 & 1 \end{pmatrix} = \begin{pmatrix} \mathbf{R} & p^* \\ 0 & 1 \end{pmatrix} \tag{16}$$

where $\mathbf{R}$ is a 3×3 direction cosine matrix equal to ($\boldsymbol{nsa}$)

as for terrestrial manipulators

$$p^* = p^*_{\mathrm{cm}} + \left(\frac{m_0}{m_\mathrm{T}}\right)\boldsymbol{s}_0 + \sum_{i=1}^{n} \mathbf{R}_i \lambda_i - \left(\frac{m_{n+1}}{m_\mathrm{T}}\right)\mathbf{R}_{n+1}\boldsymbol{r}_{n+1}$$

is the inertial position of the end-effector and

$$\lambda_i = \frac{1}{m_\mathrm{T}}\left(\sum_{j=0}^{i} m_j \boldsymbol{l}_i - m_i \boldsymbol{r}_i\right)$$

is the lumped kinematic parameter of each link i.

The DH matrix of equation (16) may be described as the Lie group SE(3) where each element is defined as a twist of the form $\mathbf{R} \in \mathrm{SE}(3) \subset \mathbf{R}^{3\times 3}$ and $p \in \mathbf{R}^3$. As each element is a twist, SE(3) may be described by the theory of screws. Forces may be represented by wrenches of screw theory such that

$$F = \begin{pmatrix} f \\ \tau \end{pmatrix} \in \mathbf{R}^{3\times 3}$$

However, Lie groups provide no additional insights into the problem presented here.

Equation (16) has the same form as that for an Earth-based manipulator of the form $p = \sum_i^n \mathbf{R}_i \boldsymbol{l}_i$ with additional constants. Note that p^*_{cm} is constant, λ_i is a lumped kinematic/dynamic parameter constant and the payload term is constant since the payload remains fixed relative to the end-effector. No loss of generality ensues by assuming that $\mathbf{R}_{n+1} = \mathbf{I}_3$ as the relative orientation of the end-effector to the object will not change. The $\boldsymbol{r}_{n+1}$ corresponds to a 'virtual stick' vector pointing from the hand of the manipulator (the manipulator grasp point) to the payload centre of mass which remains fixed in the target object [**69**]—this centre of mass of the payload is often referred to as the point of resolution (POR) for the operation of space-based manipulators such as the Shuttle RMS. The definition of this virtual stick vector in the formulation provides for a simple extension of this formulation to two manipulators forming a closed kinematic chain grasping a single object [**70**].

The same algorithms based on the DH matrix used for terrestrial manipulators can be used for computing the position of the end-effector of the robot in inertial space. This makes it possible to compute the inverse kinematics problem of determining the joint angles of the manipulator required to achieve that end-effector position in Cartesian coordinates—resolved motion control. The initialization must be recomputed on payload acquisition or release to locate the new system centre of mass in inertial coordinates, but this is a simple recomputation of the link parameters L_i in terms of the total mass and fractional mass through adding or deleting the payload mass m_{n+1}. Thus, the inverse kinematics solution to the manipulator geometry can be found with minor modifications to terrestrial algorithms, providing the desirable property of control software heritage.

Computation of end-effector velocity involves the use of the Jacobian matrix which relates end-effector velocity to joint angle rates—the Jacobian is defined by the differential relation

$$\mathbf{J}(\theta) = \frac{\partial F(\theta)}{\partial \theta}$$

The Jacobian formulation follows from the above result trivially by direct differentiation

$$v^* = \dot{p}^* = \dot{p}^*_{\mathrm{cm}} + \frac{m_0}{m_\mathrm{T}}\dot{\boldsymbol{s}}_0 + \sum_{i=1}^{n} \dot{\mathbf{R}}_i \lambda_i - \frac{m_{n+1}}{m_\mathrm{T}}\dot{\mathbf{R}}_{n+1}\boldsymbol{r}_{n+1}$$
$$= \sum_{i=1}^{n}\sum_{k=1}^{i} \frac{\partial \mathbf{R}_i}{\partial \theta_k}\lambda_i \dot{\theta}_i$$

since $\dot{p}^*_{\mathrm{cm}} = \dot{\boldsymbol{s}}_0 = \dot{\mathbf{R}}_{n+1} = 0$.

Hence

$$\overline{\mathbf{J}} = \sum_{i=1}^{n}\sum_{k=1}^{i} \frac{\partial \mathbf{R}_i}{\partial \theta_k}\lambda_i \tag{18}$$

where

$$\lambda_i = \frac{1}{m_\mathrm{T}}\sum_{j=0}^{i}(m_j \boldsymbol{l}_i - m_i \boldsymbol{r}_i)$$

In this case, there is no requirement for an initialization procedure. Thus, for a freeflying robotic manipulator employing attitude control, the freeflyer Jacobian matrix is given by [**63**, **68**]

$$\overline{\mathbf{J}} = \sum_{i=1}^{n}\sum_{k=1}^{i} \frac{\partial \mathbf{R}_i}{\partial \theta_k}\lambda_i$$

The generalized Jacobian that is applicable to free-floating systems which do not employ attitude control is given by [**36**, **44**]

$$\mathbf{J}^* = (\mathbf{J}_\mathrm{m} - \mathbf{J}_0 \mathbf{I}_0^{-1} \mathbf{D}_{ik})$$

where

$\mathbf{J}_\mathrm{m}$ = fixed base manipulator Jacobian
$\mathbf{J}_0$ = spacecraft Jacobian matrix
$\mathbf{I}_0$ = spacecraft body inertia matrix
$\mathbf{D}_{ik}$ = inertia matrix of the manipulator

The spacecraft Jacobian matrix includes both attitude and translation components so the generalized Jacobian reduces to the freeflyer Jacobian $\overline{\mathbf{J}}$ when dedicated attitude control is employed. While the generalized Jacobian is complex to compute, the freeflyer Jacobian requires only the replacement of kinematic link parameters with kinematic-dynamic parameters, and the

positional constants differentiate to zero. Hence, the Jacobian may be inverted normally as with terrestrial manipulators. This freeflyer Jacobian is much simpler to compute than the generalized Jacobian for a freefloating system without attitude control. All these new 'lumped' dynamic parameters may be precalculated offline and stored in memory, with the exception of the payload parameters which involve negligible online calculation. Furthermore, the Jacobian matrix can be determined as a byproduct of Newton–Euler dynamic analysis through the vectorial representation of velocities and angular velocities of each manipulator link [**71**]. From the Jacobian matrix it is also possible to compute resolution of acceleration between the end-effector and the manipulator joints of the form $\ddot{\boldsymbol{q}} = \mathbf{J}\ddot{\theta} + \dot{\mathbf{J}}\dot{\theta}$ [**72**]. Resolution of end-effector forces/torques to joint torques of the form $\tau = \mathbf{J}^{\mathrm{T}}\boldsymbol{F}_{\mathrm{ext}}$ may also be computed, allowing the implementation of a hybrid position/force control algorithm in conjunction with a Cartesian force/torque sensor (typically mounted in the manipulator wrist) which are essential for complex on-orbit servicing tasks [**73–75**]. The hybrid position/force control scheme divides the manipulation task into two orthogonal subspaces defined by physical motion (position) and virtual motion (force) of the end-effector through a selection matrix. The selection matrix ensures that the position and force subcontrollers do not interact. It is also possible to define a manipulability index $w = \sqrt{|\mathbf{J}\mathbf{J}^{\mathrm{T}}|}$ from the quality of the workspace at any point which can be determined from $w \geq 1/2$ [**76, 77**]. Finally, for a closed kinematic chain of two manipulators grasping a common payload, the grasp matrix can be defined on the basis of the Jacobian defined by $\mathbf{I}_{n+1}\dot{\boldsymbol{v}}_{n+1} = \bar{\mathbf{J}}^{\mathrm{T}}F$, where $\bar{\mathbf{J}}^{\mathrm{T}}$ is the grasp matrix.

6 SPACE-BASED DYNAMICS FORMULATION

The problem of computing position, velocity, acceleration and static force of the end-effector in space with respect to the manipulator joint angles, rates, accelerations and torques has been considered. It is now necessary to consider the angular component of the Denavit–Hartenburg matrix. For an attitude-controlled platform with a space manipulator, the dynamic formulation includes a moving platform with a finite translational velocity

$$v_0 = -\frac{1}{m_{\mathrm{T}}}\sum_{j=1}^{n}\sum_{i=1}^{n} m_j v_{\mathrm{c}i}$$

and this motion is compensated for within the formulations given in the previous section. When attitude control is employed, $w_0 = \dot{w}_0 = 0$, but v_0 and $\dot{v}_0$ are finite. This requires that the robot dynamics are calculated with respect to base coordinates at the manipulator/spacecraft mounting point. The translation effects on the spacecraft mounting platform owing to the movement of manipulator have been considered. It is now necessary to consider the angular effects which we regard as the moments exerted on the spacecraft by the movement of the manipulator. The reaction moments may be fed forward to the dedicated attitude control system to compensate for and cancel these moments applied to the robotic servicer. The computation of reaction moments N_{r} on the spacecraft may be determined from the generalized Jacobian formulation and the manipulator inertia matrix [**36**]

$$N_{\mathrm{r}} = -\mathbf{D}_{ik}(\mathbf{J}^*)^{-1}v^*$$

where

$\mathbf{J}^*$ = generalized Jacobian

v^* = inertial Cartesian velocity of the end-effector

However, this computation has a complexity $O(n^2)$ owing to the computation of the manipulator inertia matrix. The moments on the spacecraft that are due to manipulator movements about the coupling point at the manipulator base may alternatively be determined from the NE formulation and are given by [**54**]

$$N_{\mathrm{T}} = \sum_{i=1}^{n+1}\int p_{\mathrm{c}i} \times \ddot{p}_{\mathrm{c}i}\,\mathrm{d}m \tag{19}$$

Now, the moment about the coupling point is referred to inertial coordinates $p_{\mathrm{c}i} = p^*_{\mathrm{c}i} - r_{\mathrm{c}0} - \boldsymbol{s}_0$.

Hence

$$N_0 = \sum_{i=1}^{n+1}\int p_{\mathrm{c}i} \times (\ddot{p}^*_{\mathrm{c}i} - \ddot{r}_{\mathrm{c}0} - \ddot{\boldsymbol{s}}_0)\,\mathrm{d}m \tag{20}$$

Now, $\ddot{\boldsymbol{s}}_0 = 0$ since $\boldsymbol{s}_0$ is invariant

$$N_0 = \sum_{i=1}^{n+1}\int p_{\mathrm{c}i} \times \ddot{p}^*_{\mathrm{c}i}\,\mathrm{d}m - \sum_{i=1}^{n+1}\int p_{\mathrm{c}i} \times \ddot{r}_{\mathrm{c}0}\,\mathrm{d}m$$

For any inertially fixed frame of reference

$$\int p_{\mathrm{c}i} \times \ddot{p}^*_{\mathrm{c}i}\,\mathrm{d}m = p_{\mathrm{c}i} \times \mathrm{d}F$$

This may be substituted into equation (20)

$$N_0 = \sum_{i=1}^{n+1} p_{\mathrm{c}i} \times \mathrm{d}F - \sum_{i=1}^{n+1}\int p_{\mathrm{c}i} \times \ddot{r}_{\mathrm{c}0}\,\mathrm{d}m \tag{21}$$

Now, the total moments on each link of the manipulator are given by

$$N_{\mathrm{T}} = \sum_{i=1}^{n+1} N_{\mathrm{c}i} = \sum_{i=1}^{n+1} p_{\mathrm{c}i} \times \mathrm{d}F$$

Substitution of this into equation (21) yields

$$N_0 = N_T - \sum_{i=1}^{n+1} m_i p_{ci} \times \ddot{r}_{c0} \tag{22}$$

Now, the location of the system centre of mass is defined by

$$\begin{aligned} p^*_{cm} &= \frac{1}{m_T}\sum_{i=0}^{n+1} m_i p^*_{ci} = \frac{1}{m_T}\sum_{i=0}^{n+1}\sum_{j=i}^{n+1} m_j r_{ci} \\ &= \frac{1}{m_T}\left(\sum_{i=0}^{n+1} m_i r_{c0} + \sum_{i=1}^{n+1} m_i s_0 + \sum_{i=1}^{n+1} m_i p_{ci}\right) \\ &= r_{c0} + \frac{1}{m_T}\left[(m_T - m_0)s_0 + \sum_{i=1}^{n+1} m_i p_{ci}\right] \end{aligned}$$

Hence

$$\sum_{i=1}^{n+1} m_i p_{ci} = m_T(p^*_{cm} - r_{c0}) - (m_T - m_0)s_0 \tag{23}$$

where

$$r_{c0} = p^*_{cm} - \frac{1}{m_T}\sum_{i=1}^{n+1}\sum_{j=i}^{n+1} m_j r_{ci}$$

from equation (10).

Substitution of the summation of equation (23) yields

$$N_0 = N_T - [m_T(p^*_{cm} - r_{c0}) - (m_T - m_0)s_0] \times \ddot{r}_{c0} \tag{24}$$

Similarly, since no external forces are acting, it is possible to sum the forces acting at each link of the manipulator

$$\begin{aligned} F_T &= \sum_{i=0}^{n+1} F_{ci} = \sum_{i=0}^{n+1} m_i \ddot{p}^*_{ci} = 0 = \sum_{i=0}^{n+1}\sum_{j=i}^{n+1} m_j \ddot{r}_{ci} \\ &= \sum_{i=0}^{n+1} m_i \ddot{r}_{c0} + \sum_{i=0}^{n+1} m_i \ddot{s}_0 + \sum_{i=0}^{n+1} m_i \ddot{p}_{ci} \\ &= m_T \ddot{r}_{c0} + \sum_{i=1}^{n+1} m_i \ddot{p}_{ci} = 0 \end{aligned} \tag{25}$$

Hence

$$\ddot{r}_{c0} = -\frac{1}{m_T}\sum_{i=1}^{n+1} m_i \ddot{p}_{ci} \tag{26}$$

Now, the total reaction force on the base of the manipulator is given by

$$F_T = \sum_{i=1}^{n+1} m_i \ddot{p}_{ci} \rightarrow \ddot{r}_{c0} = -\frac{1}{m_T} F_T \tag{27}$$

Now

$$F_0 = m_0 \ddot{r}_{c0} = -\left(\frac{m_0}{m_T}\right) F_T \tag{28}$$

Substitution into equation (24) yields

$$\begin{aligned} N_0 = N_T + [&m_T(p^*_{cm} - r_{c0}) \\ &- (m_T - m_0)s_0] \times \frac{F_T}{m_T} \end{aligned} \tag{29}$$

This model provides the basis for a feedforward signal from the robot controller to the spacecraft attitude control system. The feedforward component by itself is unstable to disturbances as it is highly dependent on the accuracy of the predictive model, but the attitude control system provides the feedback component to counteract disturbances. This enables the attitude control system to compensate for the applied moments to the spacecraft such that the total moments about the satellite centre of mass sum to zero. The feedforward dynamics component with respect to local inertial coordinates is given by the reaction moments on the mounting point [**63**, **68**]:

$$N_r = N_T + (p^*_{cm} - r_{c0} - s_0) \times F_T \tag{30}$$

where

$$\begin{aligned} F_T &= \sum_{i=1}^{n+1} F_{ci} = \sum_{i=1}^{n+1} m_i \dot{v}_{ci} \\ N_T &= \sum_{i=1}^{n+1} N_{ci} = \sum_{i=1}^{n+1} \mathbf{I}_i \dot{w}_i + w_i \times \mathbf{I}_i w_i \end{aligned}$$

This gives the moments and forces on the spacecraft at the manipulator base with respect to inertial coordinates. The sum of moments about the spacecraft bus centre of mass which must be compensated for by the attitude controller is

$$\begin{aligned} N_r &= N_0 + s_0 \times F_0 \\ &= N_T + [m_T(p^*_{cm} - r_{c0}) - (m_T - m_0)s_0] \\ &\quad \times \frac{F_T}{m_T} - s_0 \times \left(\frac{m_0}{m_T}\right) F_T \\ &= N_T + (p^*_{cm} - r_{c0} - s_0) \times F_T \end{aligned}$$

The dynamics of the spacecraft platform for the attitude control system itself is given by the Euler equations

$$N_r = \mathbf{I}_0 \dot{w}_0 + w_0 \times \mathbf{I}_0 w_0 \tag{31}$$

The values of N_0 and F_0 are computed as a byproduct of the NE formulation of the manipulator dynamics in computing the required joint motor torques [**23**]. The employment of feedforward compensation to the attitude control system to stabilize the attitude of the spacecraft improves the stability of spacecraft attitude by an order of magnitude over uncontrolled attitude.

The Japanese ETS VII (1998) on-orbit servicing robotics experiment indicated that lack of attitude control while controlling the manipulator on the chaser spacecraft was subject to many problems—without compensating for attitude reaction torques, the attitude error became large [**78**]. This was primarily because the spacecraft is not symmetric owing to the robotic configuration, so gravity gradient torques generated by the products of inertia were non-negligible which in turn depended on the attitude error of the system. Hence, active dedicated attitude control of the platform is essential.

This completes the present approach to simplifying the dynamic equations enabling control of the robot manipulator in space with marginal increases in computational complexity over terrestrial manipulator systems. Indeed, the same algorithms such as the RCCL may be used with marginal modification—a simple subroutine to compute the link parameters and their masses as lumped parameters.

7 SIMULATION RESULTS

The case study that has been selected is the ATLAS (Advanced TeLerobotic Actuation System) servicer concept which represents a realistic robotic servicer concept (Fig. 2) [**60**, **63**]. ATLAS has the physical properties shown in Table 1 (assuming a single six-degree-of-freedom manipulator) [**60**, **63**].

The manipulator on ATLAS has a PUMA 560/600 kinematic configuration. All on-orbit servicing tasks involve a complex sequence of basic movements (primitives), e.g. move, approach, grapple, yield, insert and extract (the last four primitives require force control) which may be assembled into more generic tasks such as open hatch, close hatch, install ORU, remove ORU, etc. The ATLAS servicer is modelled grappling a 200 kg orbital replacement unit (ORU)—this models the attitude control module (ACM) of the multimodular spacecraft (MMU). The Solar Maximum spacecraft was based on the MMU, and the Solar Maximum repair mission of 1984 is considered a 'textbook' servicing mission which comprised two fundamental tasks performed by astronauts of the STS-41C mission. The first task for the Solar Maximum repair mission, which is of interest here, was the ACM replacement which was a well-defined and well-characterized task eminently suited to simple servicing tasks. The second task, which was much more complex, was the main electronics box (MEB) replacement, which is not considered further—indeed, it has never been replicated robotically. It is not of present concern to model the complete servicing task as this is highly complex and many of the tasks are variations on the 'peg-in-hole' operation which can be broken down into force and position controlled subtasks [**79**]. The concern here is to determine the torques imposed on the spacecraft by the movements of the manipulator arms during two phases of the manipulator deployment during the acquisition of the ACM:

1. Manipulator movement to acquire the ACM. The manipulator is position controlled and has no payload.
2. Manipulator grappling of the ACM on acquisition. The manipulator is force controlled to passivate the ACM.

These types of maneouvre are fundamental to on-orbit servicing. DLR (Deutschen Zentrum für Luft- und Raumfahrt), the German Space Agency, has also developed a specialized capture for this purpose [**80**]. The DLR capture tool comprises six laser rangefinders, a force–torque sensor and a stereocamera pair to provide the sensor component to their teleprogramming approach to autonomous insertion and capture of the apogee kick motor of a geostationary satellite platform. The reaction torques were modelled as a torque trajectory over time through a series of knot points which represent control points. The computed torque

Table 1 Physical properties of ATLAS

Kinematic chain	Mass (kg)
Link 0 (spacecraft bus)	1000
Link 1 (manipulator shoulder)	8
Link 2	6
Link 3 (manipulator elbow)	6
Link 4	0
Link 5 (manipulator wrist)	12
Link 6 (manipulator end effector)	8
Link 7 (payload)	200

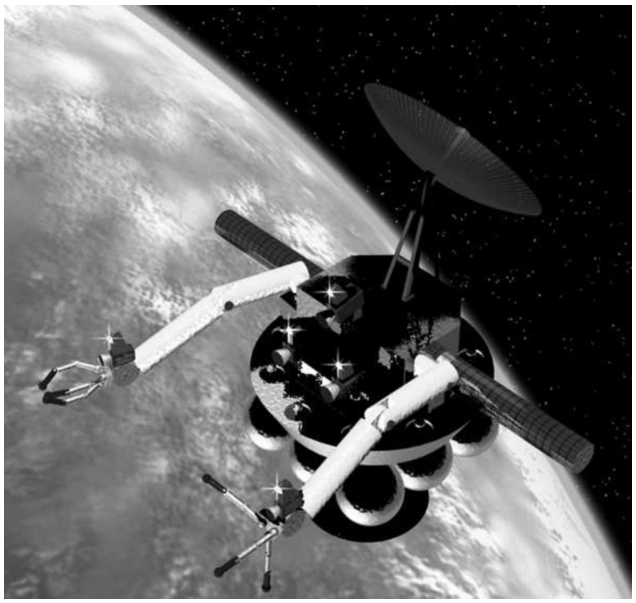

Fig. 2 ATLAS robotic servicer (courtesy Praxis Publishers)

control law, a linearized feedforward model-based PD feedback control system based on inverse dynamics, was adopted for the manipulator position control [**81**]

$$\ddot{\theta}_i = \ddot{\theta}_i^{\mathrm{d}} + \sum_{j=1}^{n} K_v^{ij}\left(\dot{\theta}_j^{\mathrm{d}} - \dot{\theta}_j\right) + \sum_{j=1}^{n} K_{\mathrm{p}}^{ij}\left(\theta_j^{\mathrm{d}} - \theta_j\right) \qquad (31)$$

Although flexural dynamics is not of specific concern here, it is worth pointing out that rigid body control schemes such as the computed torque method will actively damp out vibrations to some extent through the proper adjustment of rate feedback gains and the control of manoeuvre speed [**12**, **82**, **83**]. Alternative methods of manipulator control may be adaptive techniques [**84**, **85**] or optimal controllers [**86**], but the computed torque method does provide robust [**87**] and adaptive properties [**88**] to compensate for unmodelled aspects of the system. The end-effector trajectory can be divided up into N segments of equal time $t_s = T/N$, where T is the total manoeuvre time. Each segment can be approximated by a cubic polynomial interpolation function such that control is linear across each segment. The control algorithm here was computed at six knot points defined by a start position (initial configuration, zero velocity, maximum acceleration) to a final position (final configuration, zero velocity, maximum deceleration) in a bang-bang manoeuvre (no coasting phase). The force control law adopted was a linearized PI feedback control system of the form

$$\tau_f = \mathbf{J}^T f_{\mathrm{ext}}^{\mathrm{d}} + K_{\mathrm{F}}\left(f_{\mathrm{ext}}^{\mathrm{d}} - f_{\mathrm{ext}}\right) + K_{\mathrm{F}i}\int\left(f_{\mathrm{ext}}^{\mathrm{d}} - f_{\mathrm{ext}}\right)\mathrm{d}t$$

The external forces were generated by the impact dynamics. Such impacts may range from fully plastic to fully elastic [**88**]. A plastic impact involves two bodies becoming rigidly attached to each other after impact while conserving momentum. An elastic impact involves two bodies rebounding without the loss of energy. The impact duration was modelled as 10^{-3} s which is much less than the period of the fundamental mode of vibration of the manipulator links, so deflection of the manipulator from its nominal configuration was assumed to be negligible. Assuming that impact occurs at a single point on the end-effector, and that momentum is conserved before the impact at time t and after impact at time $t+1$, a plastic impact has the following force and torque

$$\boldsymbol{F}_{\mathrm{ext}} = F_{n+1} = m_{n+1}\dot{v}_{n+1} = m_{n+1}\left(\frac{v_{t+1} - v_t}{\delta t}\right)$$

$$\boldsymbol{N}_{\mathrm{ext}} = I_{n+1}\dot{w}_{n+1} = r_{n+1} \times F_{n+1} = I_{n+1}\dot{w}_{n+1} = I_{n+1}\left(\frac{w_{t+1} - w_t}{\delta t}\right)$$

where

F_{n+1} = impact force exerted by the payload

r_{n+1} = lever arm between the end-effector and the centre of mass of the payload ('virtual stick')

Passivation of the final configuration to zero relative velocity is determined by the external forces and torques on the end-effector imposed by the payload. The force control phase for passivation was computed with as many knot points as required to reach a passivation level of near-zero reaction torques—this was dependent on the force control gains which may be adjusted to yield any desired torque trajectory, but present interest is primarily in the initial reaction torques imposed at impact. An analysis was made of the reaction moments generated on the spacecraft platform for relative end-effector collision velocities of 0.1 and 1 m/s to simulate a bias rotational velocity of the target (spin). The lower end of collision velocities is similar to the closing velocities for US and Russian impact docking manoeuvres of 0.05–0.1 m/s.

The reaction moments on the spacecraft bus using the computed torque control law prior to acquisition of the target are fairly low < 5 N m (Fig. 3). This correlates reasonably well with the peak angular momentum of 10 N m/s due to manipulator motions experienced by ETS VII [**78**]. These reaction torques are large, however, in comparison with the typical attitude disturbance torques experienced by spacecraft in microgravity $\sim 10^{-6}$–10^{-3} N m from orbit perturbations. Furthermore, these moments are barely within the bounds of the capabilities of reaction wheels which are generally limited to $\sim$0.1–1 N m torques typically [**57**].

The reaction torques on the spacecraft bus while implementing force control of the manipulator during target acquisition and subsequent passivation are high $\sim$1–10 kN m (Fig. 4). This correlates well with commonly experienced in-space docking forces of $\sim$1–5 kN (depending on the lever arm from the centre of mass). These torques are far in excess of the capabilities of reaction wheels to compensate, but control moment gyroscopes (CMGs) do have sufficient torque capability (for example, the ISS CMGs have maximum torque capabilities of 27 kN m). Clearly, force control is a

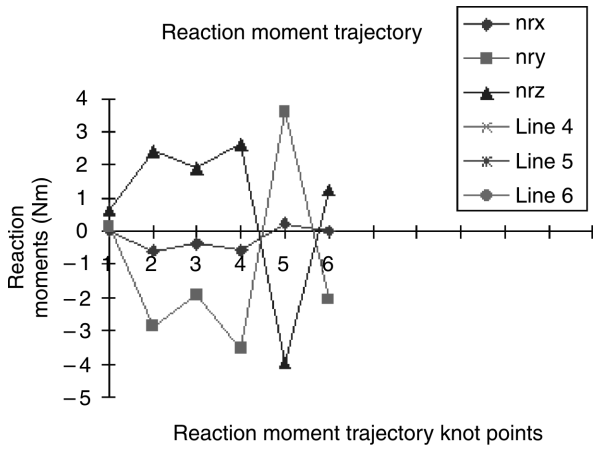

Fig. 3 Reaction moments for the computed torque control law prior to target acquisition

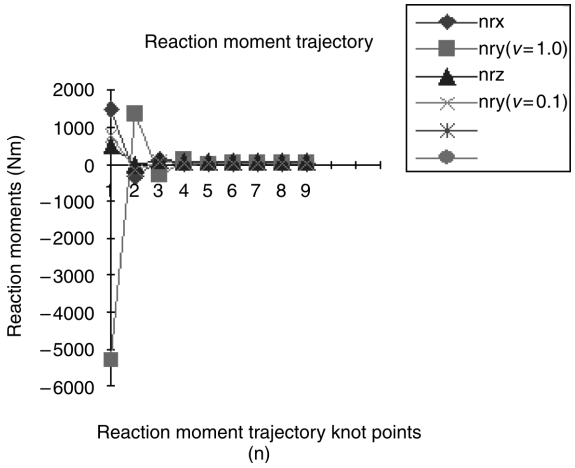

Fig. 4 Reaction moments for the force control law on target acquisition

critical capability in robotic on-orbit servicing. The results from simulation studies indicate that the exerted reaction torques on the spacecraft platform will require the implementation of control moment gyroscopes, as reaction wheels cannot provide sufficient moment compensation to the spacecraft platform [**63**].

8 CONCLUSIONS

This completes the kinematics and dynamics of a single-manipulator spacecraft treated as a kinematic chain. The further advantage is that this formulation represents a natural approach from the spacecraft engineering viewpoint—the separate treatment of linear and angular momentum is fundamentally achieved in the design of spacecraft subsystems such that the orbit manoeuvres and attitude of the spacecraft are engineered separately through a dedicated orbital transfer subsystem and attitude control subsystem. Furthermore, this formulation does not suffer from the problems of unpredictable dynamic singularities in the manipulator workspaces as a direct result of the non-holonomy of attitude control [**37**, **42**]. Control becomes unstable in these regions which, unlike in their terrestrial counterpart, cannot be predicted as they are functions of both kinematic geometry and the dynamics of the robotic manipulator. Such freefloating systems do not employ dedicated attitude control systems (which nonetheless would be required onboard a spacecraft for station-keeping) but utilize a 'coning' motion to control attitude [**31**, **34**]—a hazardous notion for on-orbit servicing proximity operations at best.

The formulation may be readily extended to more than one manipulator which would be modelled as a branched kinematic chain [**63**]. This formulation can also be extended to account for closed-chain configurations of two manipulators holding a single payload which defines a common reference frame. This simple model encapsulates the most important aspects in deriving real-time control laws for a robotic freeflyer spacecraft. This enables the onboard control system to compensate for manipulation of objects and targets in zero gravity, automatically compensating for reaction effects on itself. Furthermore, computer simulation suggests that the implementation of force control will require the use of powerful attitude actuators, namely control moment gyroscopes, as only these devices have torque outputs sufficient to stabilize the spacecraft platform against the high reaction disturbance torques.

This work has considerable implications for the design of robotic on-orbit servicing freeflyer platforms that are currently envisaged for servicing of current and future space assets [**90**, **60**].

ACKNOWLEDGEMENTS

The author acknowledges the support for most of this work that was provided by the College of Aeronautics at Cranfield University under EPSRC research studentship funding. Elie Allouis and Vincent Shaw-Morton are thanked for producing the images.

REFERENCES

1 **Ellery, A., Welch, C.** and **Curley, A.** A proposed public–private partnership for the funding of robotic in-orbit servicers. In ASME Proceedings of Space and Robots Conference 2002, Alburquerque, New Mexico, March 2002.
2 **Shrivastava, S.** and **Modi, V.** Satellite attitude dynamics and control in the presence of environmental torques—a brief survey. *J. Guidance*, 1983, **6**(6), 461–471.
3 **Marcyk, J.** and **Bellazzi, A.** Dynamics and control of freeflying inspection and maintenance vehicle with manipulators. In Proceedings of 2nd European In-Orbit Operations Technology Symposium, 1989, ESA SP-297, pp. 413–427.
4 **Hooker, W.** and **Margulies, G.** Dynamical attitude equations for *n*-body satellite. *J. Astronaut. Sci.*, 1965, **12**(4), 123–128.
5 **Hooker, W.** Set of *r* dynamical attitude equations for arbitrary *n*-body satellite with *r* rotational degrees of freedom. *Am. Inst. Aeronaut. Astronaut. J.*, 1970, **8**(7), 1205–1207.
6 **Ho, J.** Direct path method for flexible multibody spacecraft dynamics. *J. Space*, 1977, **14**(2), 102–110.
7 **Jerkovsky, W.** Structure of multibody dynamics equations. *J. Guidance and Control*, 1978, **1**(3), 173–182.
8 **Hughes, P.** Dynamics of a chain of flexible bodies. *J. Astronaut. Sci.*, 1979, **27**(4), 359–380.
9 **Grewal, A.** and **Modi, V.** Dynamics and control of multibody systems: an approach with applications. *Acta Astronaut.*, 1996, **39**(5), 323–346.

10 **Grewal, A.** and **Modi, V.** Robust attitude and vibration control of the Space Station. *Acta Astronaut.*, 1996, **38**(3), 139–160.

11 **Van Woerkom, P.** Synthesis and summary of control laws for large flexible spacecraft. *Control Theory and Advd Technol.*, 1993, **9**(3), 639–669.

12 **Goel, P.** and **Maharama, P.** Active damping technique for satellites with flexible appendages. *Acta Astronaut.*, 1995, **36**(5), 239–250.

13 **Murotsu, Y., Tsujio, S., Senda, K.** and **Hayashi, M.** Trajectory control of flexible manipulators on a freeflying space robot. *IEEE Control Syst.*, June 1992, 51–57.

14 **Van Woerkom, P.** and **Misra, A.** Robotic manipulators in space: a dynamics and control perpective. *Acta Astronaut.*, 1996, **38**(4–8), 418–421.

15 **Paul, R.** Robot manipulators: mathematics, programming and control (MIT Press, Cambridge, Massachusetts).

16 **Fu, K., Gonzalez, R.** and **Lee, C.** *Robotics: Control, Sensing, Vision and Intelligence*, 1987 (McGraw-Hill, Singapore).

17 **Rodriguez, G.** Kalman filtering, smoothing and recursive robot arm forward and inverse dynamics. *IEEE J. Robotics and Automn*, 1987, **3**(6), 624–639.

18 **Johnson, D.** and **Hill, J.** Kalman filter approach to sensor based robot control. *IEEE J. Robotics and Automn*, 1985, **1**(3), 159–162.

19 **Silver, W.** On equivalence of Lagrangian and Newton–Euler dynamics for manipulators. *Int. J. Robotics Res.*, 1982, **1**(2), 60–69.

20 **Walker, M.** and **Orin, D.** Efficient dynamic computer simulation of robotic mechanisms. *Trans. ASME, J. Dynam Syst. Mechanics and Control*, September 1982, **104**, 205–211.

21 **Lumia, R.** and **Wavering, A.** Trajectory generation for space telerobots. In Proceedings of NASA Workshop on *Space Telerobotics II*, 1989, pp. 123–131.

22 **Khatib, O.** Unified approach for motion and force control of robotic manipulators: operational space formulation. *Trans. ASME, Basic Engr*, March 1987, 35–45.

23 **Luh, J., Walker, M.** and **Paul, R.** On-line computational scheme for mechanical manipulators. *Trans. ASME, J. Dynamic Syst. Measmt and Control*, June 1980, **102**, 69–76.

24 **Jain, A.** and **Rodriguez, G.** Recursive flexible multibody dynamics using spatial operators. *J. Guidance, Control and Dynamics*, 1992, **15**(6), 1453–1466.

25 **Van Woerkom, P.** and **De Boer, A.** Development and validation of a linear recursive 'order *n*' algorithm for the simulation of flexible space manipulator dynamics. *Acta Astronaut.*, 1995, **35**(2/3), 175–185.

26 **Hollerbach, J.** Recursive Lagrangian formulation of manipulator dynamics and comparative study of dynamics formulation complexity. *IEEE Trans. Syst. Man and Cybernetics*, 1980, **10**(11), 730–736.

27 **Kane, T.** and **Levinson, D.** Formulation of equations of motion for complex spacecraft. *J. Guidance and Control*, 1983, **6**(2), 99–122.

28 **Nagashima, F.** and **Nakaruma, Y.** Efficient computation scheme for the kinematics and inverse dynamics of a satellite-based manipulator. In Proceedings of IEEE International Conference on *Robotics and Automation*, 1992, pp. 905–912.

29 **Kane, T.** and **Levinson, D.** Use of Kane's equations in robotics. *Int. J. Robotics Res.*, 1983, **2**(3), 3–21.

30 **Konigstein, R.** Computed torque control of freeflying cooperating arm robot. In Proceedings of NASA Workshop on *Space Telerobotics V*, 1989, pp. 235–243.

31 **Longman, R.** Kinetics and workspace of robot mounted on satellite that is free to rotate and translate. AIAA 88-4097-CP, 1988.

32 **Vafa, Z.** and **Dubowsky, S.** On dynamics of manipulators in space using the virtual manipulator approach. In Proceedings of IEEE International Conference on *Robotics and Automation*, 1987, pp. 579–585.

33 **Vafa, Z.** and **Dubowsky, S.** Kinematics and dynamics of space manipulators: the virtual manipulator approach. *Int. J. Robotics Res.*, 1990, **9**(4), 852–872.

34 **Yamada, K.** and **Yoshikawa, S.** Feedback control of space robot attitude by cyclic cone motions. *J. Guidance, Control and Dynamics*, 1997, **20**(4), 715–720.

35 **Vafa, Z.** Space manipulator motions with no satellite attitude disturbances. In Proceedings of IEEE International Conference on *Robotics and Automation*, 1990, pp. 1770–1775.

36 **Umetani, Y.** and **Yoshida, K.** Resolved motion rate control of space manipulators using a generalised Jacobian matrix. *IEEE Trans. Robotics and Automn*, 1989, **5**(3), 303–314.

37 **Papadopoulos, E.** and **Dubowsky, S.** On the nature of control algorithms for free-floating manipulators. *IEEE Trans. Robotics and Automn*, 1991, **7**(6), 750–758.

38 **Papadopoulos, E.** and **Dubowsky, S.** Coordinated manipulator/spacecraft motion control for space robotic systems. In Proceedings of IEEE International Conference on *Robotics and Automation*, 1991, pp. 1696–1702.

39 **Masutani, Y., Mayazako, F.** and **Arimoto, S.** Sensory feedback control for space manipulators. In Proceedings of IEEE International Conference on *Robotics and Automation*, 1989, pp. 1346–1351.

40 **Xu, Y.** Measure of dynamic coupling of space robot system. In Proceedings of IEEE International Conference on *Robotics and Automation*, 1993, pp. 615–620.

41 **Kowano, I., Mokuno, M., Kasai, T.** and **Suzechi, T.** Result of autonomous rendezvous docking experiment of ETS VII. *J. Spacecraft and Rockets*, 2001, **38**(1), 105–111.

42 **Papadopoulos, E.** and **Dubowsky, S.** On dynamic singularities in the control of free-floating manipulators. *Trans. ASME, Dynamic Syst. and Control*, 1989, **15**, 45–52.

43 **Papadopoulos, E.** and **Dubowsky, S.** Kinematics, dynamics and control of freeflying and freefloating space robotic systems. *IEEE Trans. Robotics and Automn*, 1993, **9**(5), 531–543.

44 **Nakaruma, Y.** and **Mukherjee, R.** Nonholonomic path planning of space robots visa the bidirectional approach. *IEEE Trans. Robotics and Automn*, 1989, **7**(4), 500–514.

45 **Nenchev, D., Umetani, Y.** and **Yoshida, K.** Analysis of a redundant freeflying spacecraft manipulator system. *IEEE Trans. Robotics and Automn*, 1992, **8**(1), 1–6.

46 **Dubowsky, S., Vance, E.** and **Torres, M.** Control of space manipulators subject to spacecraft attitude control control saturation limits. In Proceedings of NASA Workshop on *Space Telerobotics IV*, 1989, pp. 409–418.

47 **Spofford, J.** and **Akin, D.** Redundancy control of freeflying telerobots. AIAA 88-4094-CP, 1988.

48 Slotine, J.-J. and **Li, W.** On the adaptive control of manipulators. *Int. J. Robotics Res.*, 1987, **6**(3), 49–59.

49 Papadopoulos, E. and **Dubowsky, S.** On the nature of control algorithms for space manipulators. In Proceedings of IEEE International Conference on *Robotics and Automation*, 1990, pp. 1102–1108.

50 Walker, M. and **Wee, L.** Adaptive control of space based robot manipulator. *IEEE Trans. Robotics and Automn*, 1991, **7**(6), 828–835.

51 Walker, M. and **Wee, L.** Adaptive control strategy for space based robot manipulators. In Proceedings of IEEE Conference on *Robotics and Automation*, 1991, pp. 1673–1680.

52 Rui, C., Kolmanovsky, I. and **McClamroch, N.** Nonlinear attitude and shape control of spacecraft with articulated appendages and reaction wheels. *IEEE Trans. Autom. Control*, 2000, **45**(8), 1455–1469.

53 Lindberg, R., Longman, R. and **Zedd, M.** Kinematics and reaction moment compensation for the spaceborne elbow manipulator. AIAA 86-0250, 1986.

54 Longman, R., Lindberg, R. and **Zedd, M.** Satellite-mounted robot manipulators—new kinematics and reaction compensation. *Int. J. Robotics Res.*, 1987, **6**(3), 87–103.

55 Yoshida, K. Dual arm coordination of a space freeflying robot. In Proceedings of IEEE International Conference on *Robotics and Automation*, 1992, pp. 899–904.

56 Murphy, S., Wen, S. and **Saridis, G.** Simulation of cooperating robot manipulators on a mobile platform. *IEEE Trans. Robotics and Automn*, 1991, **7**(4), 468–477.

57 Mitsuskige, O. Motion control of the satellite mounted robot arm which assures satellite attitude stability. *Acta Astronaut.*, 1997, **41**(11), 739–750.

58 Nagata, T., Modi, V. and **Matsuo, H.** Dynamics and control of flexible multibody systems. Part I: general formulation with an order *n* forward dynamics. *Acta Astronaut*, 2001, **49**(11), 581–594.

59 Nagata, T., Modi, V. and **Matsuo, H.** Dynamics and control of flexible multibody systems. Part II: simulation code and parametric studies with nonlinear control. *Acta Astronaut.*, 2001, **49**(11), 595–610.

60 Ellery, A. *An Introduction to Space Robotics*, Praxis–Springer Series on Astronomy and Space Sciences, 2000 (Prais Publishers).

61 Gasbarri, P. A two dynamical approach to multibody force dynamics in the space environment. *Acta Astronaut.*, 2002, **51**(12), 831–842.

62 Krishnan, S. and **Vadali, S.** An inverse-free technique for attitude control of spacecraft using CMGs. *Acta Astronaut.*, 1996, **39**(6), 431–438.

63 Ellery, A. Systems design and control of a freeflying space robotic manipulator system (ATLAS) for in-orbit servicing operations. PhD thesis, Cranfield Institute of Technology (now Cranfield University), 1996.

64 Piper, G. and **Kwatny, H.** Complicated dynamics in spacecraft attitude control systems. *J. Guidance, Control and Dynamics*, 1992, **15**(4), 825–831.

65 Clohessy, W. and **Wiltshire, R.** Terminal guidance system for satellite rendezvous. *J. Aerospace Sci.*, 1960, **27**, 653–658.

66 Denavit, J. and **Hartenburg, R.** Kinematics notation for lower pair mechanisms based on matrices. *Trans. ASME, J. Appl. Mechanics*, 1955, **77**, 215–221.

67 Murray, R., Li, Z. and **Sastry, S.** *A Mathematical Introduction to Robotic Manipulation*, 1994 (CRC Press).

68 Ellery, A. Resolved motion control of space manipulators. In Proceedings of 45th IAF Congress, Tel Aviv, Israel, 1994, ST 94-W2-574.

69 Uchiyama, M. and **Dauchez, P.** Symmetric hybrid position/force control scheme for the coordination of two robots. In Proceedings of IEEE International Conference on *Robotics and Automation*, 1988, pp. 351–356.

70 Zheng, Y. and **Luh, J.** Optimal load distribution for two industrial robots handling a single object. In Proceedings of IEEE International Conference on *Robotics and Automation*, 1988, pp. 344–349.

71 Whitney, D. Mathematics of coordinated control of prosthetic arms and manipulators. *Trans. ASME, Dynamic Syst. Measmt and Control*, 1972, **122**, 303–309.

72 Luh, J., Walker, M. and **Paul, R.** Resolved acceleration control of mechanical manipulators. *IEEE Trans. Autom. Control*, 1980, **25**(3), 236–241.

73 Raibert, M. and **Craig, J.** Hybrid position/force control of manipulators. *Trans. ASME, Energy Res. Technol.*, June 1981, **102**, 126–133.

74 Zheng, Y. and **Paul, R.** Hybrid control of robot manipulators. In Proceedings of IEEE International Conference on *Robotics and Automation*, 1985, pp. 602–606.

75 Goldenberg, A. and **Song, P.** Principles for the design of position and force controllers for robot manipulators. *Robotics and Autonom. Syst.*, 1997, **21**, 263–277.

76 Paul, R. and **Stevenson, C.** Kinematics of robotic wrists. *Int. J. Robotics Res.*, 1983, **2**(1), 31–38.

77 Yoshikawa, T. Manipulability and redundancy control of robotic machines. In Proceedings of IEEE Conference on *Robotics and Automation*, 1985, pp. 1004–1009.

78 Oda, M. Attitude control experiments of a robot satellite. *J. Spacecraft and Rockets*, 2000, **37**(6), 788–793.

79 Backes, P. and **Tso, K.** Autonomous single arm ORU changeout—strategies, control issues and implementation. *Robotics and Autonom. Syst.*, 1990, **6**, 221–241.

80 Landzettal, K., Brunner, B., Hirzinger, G., Lampariello, R., Schenker, G. and **Stainmetz, B.-M.** Unified ground control and programming methodology for space robotics applications—demonstration on ETS VII. In Proceedings of 3rd International Symposium on *Robotics*, Montreal, Canada, 14–17 May 2000.

81 Moya, M. and **Seraji, H.** Robot control systems: a survey. *Robotics and Autonom. Syst.*, 1987, **3**, 329–351.

82 Boutin, B., Misra, A. and **Modi, V.** Dynamics and control of variable geometry truss structures. *Acta Astronaut.*, 1999, **45**(12), 717–728.

83 Spong, M. Adaptive control of flexible joint manipulators: comments on two papers. *Automatica*, 1995, **31**(4), 585–590.

84 Van Woerkom, P., Guelman, M. and **Ehrenwald, L.** Integrated adaptive control for space manipulators. *Acta Astronaut.*, 1996, **38**(3), 161–174.

85 Ehrenwald, L. and **Guelman, M.** Stability and convergence of integrated adaptive control for space manipulators. *Robotics and Autonom. Syst.*, 1996, **19**, 151–166.

86 Cornerstone-Carrol, V. and **Wilking, N.** Optimal control of a satellite–robot system using direct collocation with nonlinear programming. *Acta Astronaut.*, 1995, **36**(3), 149–162.

87 Abdullah, C. Survey of robust control for rigid robots. *IEEE Control Syst*., February 1991, 24–29.
88 Astrom, K. Adaptive feedback conrol. *Proc. IEEE*, 1987, **75**(2), 185–217.
89 Xavier, C., Sun-Wook, K., Ingham, M., Miora, A. and **Gilbert, J.** Post-impact dynamics of two multi-body systems attempting docking/berthing. *Acta Astronaut*., 1997, **40**(11), 759–769.
90 Waltz, D. *On-Orbit Servicing of Space Systems*, 1993 (Krieger, Florida).
91 McInnes, C. Optimum orbit selection for two-vehicle rendezvous. *ESA J*., 1992, **16**, 447–454.

APPENDIX

Clohessy–Wiltshire equations

The Clohessy–Wiltshire equations for phasing orbit manoeuvres are computed with respect to local inertial coordinates. The relative position vector representing the separation of a target spacecraft T and a chaser spacecraft C (typically within 100 km of each other) is small in comparison with the target orbit radius R, where $R = R_E + h$, $R_E =$ Earth's radius $= 6378$ km and $h =$ orbital altitude $= 200$–500 km for low Earth orbit. It is thus acceptable to use a moving coordinate frame of reference located at the target spacecraft. The rendezvous phase prior to docking of the robotic servicer spacecraft (the chaser) and the target satellite is described by the Clohessy–Wiltshire equations which determine the relative motion of the two spacecraft in close proximity. Closed-form solutions give the velocities required to coast to rendezvous within a specified time for circular orbits [**65**].

Horizontal acceleration,

$$a_x = \ddot{x} - 2w_0\dot{z}$$

Vertical acceleration

$$a_z = \ddot{z} - 3w_0^2 z + 2w_0\dot{x}$$

where the orbital velocity $w_0 = \sqrt{GM_E/R^3}$.

Closed-form solutions exist for $a_x = a_z = 0$

$$x(t) = -2\left(\frac{\dot{z}_0}{w_0}\right)\cos w_0 t + \left[4\left(\frac{\dot{x}_0}{w_0}\right) - 6z_0\right]\sin w_0 t + \left[6z_0 - 3\left(\frac{\dot{x}_0}{w}\right)\right]w_0 t + x_0 + 2\left(\frac{\dot{z}_0}{w_0}\right)$$

$$z(t) = \left[2\left(\frac{\dot{z}_0}{w_0}\right) - 3z_0\right]\cos w_0 t + \left(\frac{\dot{z}_0}{w_0}\right)\sin w_0 t + 4z_0 - 2\left(\frac{x\dot{z}_0}{w_0}\right)$$

where (x_0, z_0) is the initial orbital position with respect to the target.

The Clohessy–Wiltshire equations provided the basis for the Japanese Engineering Test Satellite VII (1998) mission [**41**] and these may be incorporated into potential field formulations that provide for orbit manoeuvres in close proximity to other space vehicles [**91**]. ETS VII comprised two satellites—a chaser and a target—to demonstrate rendezvous, docking and on-orbit servicing tasks in a 550 km altitude orbit inclined at 35°. The chaser approached the target in order to dock with it from a separation distance of 12 km using GPS navigation for coarse navigation and laser radar and video cameras for proximity navigation. The docking process was cooperative, involving manoeuvres from both spacecraft—this would in general not be the case for robotic on-orbit servicers. TDRSS was used for the communications relay to the ground. There were three navigation phases: a relative approach phase from 12 km to 500 m using GPS, the final approach phase from 500 to 2 m using laser radar and the docking phase from 2 m to contact using the cameras. Low closing velocities of 0.01 m/s were adopted which required high control effort. Orbit control was performed by thrusters and the high control effort required many thruster firings at intervals of 1–3 s. Three reaction wheels were used to provide spacecraft attitude control augmented by thrusters for angular momentum dumping of saturated wheels. In the relative approach phase, the chaser used the Clohessy–Wiltshire equations for guidance. On grappling of the target, the chaser's manipulator captured the target latching port at a top speed of 0.02 m/s for low impact docking which generated peak accelerations of $< 9\,\text{mm/s}^2$—these are much lower than those described in the simulation as the ETS VII demonstrator mission involved a cooperative target.